

# Coupled Bootstrap Test Error Estimation for Poisson Variables

Natalia L. Oliveira<sup>1,2</sup>

Jing Lei<sup>1</sup>

Ryan J. Tibshirani<sup>1,2</sup>

<sup>1</sup>Department of Statistics and Data Science, <sup>2</sup>Machine Learning Department  
Carnegie Mellon University

## Abstract

Test error estimation is a fundamental problem in statistics and machine learning. Correctly assessing the future performance of an algorithm is an essential task, especially with the development of complex predictive algorithms that require data-driven parameter tuning. We propose a new coupled bootstrap estimator for the test error of Poisson-response algorithms, a fundamental model for count data and with applications such as signal processing, density estimation, and queue theory. The idea behind our estimator is to generate two carefully designed new random vectors from the original data, where one acts as a training sample and the other as a test set. It is unbiased for an intuitive parameter: the out-of-sample error of a Poisson random vector whose mean has been shrunk by a small factor. Moreover, in a limiting regime, the coupled bootstrap estimator recovers an exactly unbiased estimator for test error. Our framework is applicable to loss functions of the Bregman divergence family, and our analysis and examples focus on two important cases: Poisson likelihood deviance and squared loss. Through a bias-variance decomposition, we analyze the effect of the number of bootstrap samples and the added noise due to the two auxiliary variables. We then apply our method to different scenarios with both simulated and real data.

## 1 Introduction

We consider the problem of estimating the out-of-sample error of a mean estimator on a sequence of Poisson random variables, called the *many Poisson means problem* or *Poisson compound problem*. We observe a data vector  $Y = (Y_1, \dots, Y_n)$  with independent entries  $Y_i \sim \text{Poisson}(\mu_i)$ , and  $\mu = (\mu_1, \dots, \mu_n) \in \mathbb{R}_+^n$  is an unknown vector of parameters to be estimated. Let  $g : \mathbb{N}_0^n \rightarrow \mathbb{R}_+^n$  be a measurable function that estimates  $\mu$  from data  $Y$ , that is,  $\hat{\mu} = g(Y)$ . To evaluate the performance of  $g$ , its out-of-sample error (or test error)  $\text{Err}(g)$  for loss function  $\ell : \mathbb{N}_0^n \times \mathbb{R}_+^n \rightarrow \mathbb{R}_+$  is

$$\text{Err}(g) = \mathbb{E}[\ell(\tilde{Y}, g(Y))],$$

where  $\tilde{Y}$  is an i.i.d. sample of  $Y$ . The out-of-sample error  $\text{Err}(g)$  measures how well  $g(Y)$  predicts new observations  $\tilde{Y}$ .

A sub-case of the many Poisson means framework is fixed- $X$  Poisson regression. In this case,  $Y \in \mathbb{N}_0^n$  is a response variable,  $X \in \mathbb{R}^{n \times p}$  is a *fixed* feature matrix, and  $g$  is any regression function that maps  $(Y, X)$  to a predicted vector of  $Y$ . Fixed- $X$  means that it is a common feature matrix for both training  $(Y, X)$  and test sets  $(\tilde{Y}, X)$ . When there is an interest in evaluating the performance of  $g$  on a test set whose feature matrix is different from the training features, the *random- $X$*  framework is more appropriate, which is *not* equivalent to the many Poisson means problem and therefore not contemplated in this paper.

### 1.1 Error estimation and risk estimation

Risk is defined as the expected loss between  $g(Y)$  and the parameter of interest  $\mu$

$$\text{Risk}(g) = \mathbb{E}[\ell(\mu, g(Y))].$$

While test error measures how well  $g$  predicts a new sample  $\tilde{Y}$ , risk measures how well  $g$  estimates  $\mathbb{E}[Y] = \mathbb{E}[\tilde{Y}] = \mu$ . Intuitively these quantities seem related: a  $g$  with low risk should also have low test error. We formally characterize this relationship for the Bregman divergence family of loss functions.

Let  $D_\phi(x_1, x_2)$  be the Bregman divergence loss defined by

$$D_\phi(x_1, x_2) = \phi(x_1) - \phi(x_2) - \phi'(x_2)(x_1 - x_2),$$

where  $\phi$  is a convex function that characterizes the the loss. For instance,  $\phi(x) = x^2$  and  $\phi(x) = 2x(\log x - 1)$  reduce  $D_\phi$  to the squared loss and deviance loss, respectively.

Assuming  $\ell$  is a Bregman divergence loss with convex function  $\phi$  and  $\mathbb{E}[Y] = \mu$ ,

$$\text{Err}(g) - \text{Risk}(g) = \mathbb{E}[\phi(Y) - \phi(\mu)]. \quad (1)$$

The RHS of Equation (1) is Jensen’s gap. Note that this quantity does not depend on  $g$ ; therefore, if we have an estimator for out-of-sample error, we are automatically able to estimate risk up to a constant, so the out-of-sample error and risk are equivalent in tasks such as model comparison and tuning parameter selection. Throughout this paper, we will focus on estimating out-of-sample error, but all results are also valid for risk-up-to-constant (and risk exactly at least in the squared loss setting).

## 1.2 Deviance vs squared loss

We will focus on two loss functions in the family of Bregman divergence loss functions: Poisson deviance and squared loss.

$$\begin{aligned} \text{Err}^{(\text{Sqr})}(g) &= \mathbb{E}[\|\tilde{Y} - g(Y)\|_2^2], \\ \text{Err}^{(\text{Dev})}(g) &= \mathbb{E}\left[2 \sum_{i=1}^n \tilde{Y}_i \log \frac{\tilde{Y}_i}{g_i(Y)} + g_i(Y) - \tilde{Y}_i\right], \end{aligned}$$

where  $g_i(Y)$  denotes the  $i$ th component of  $g(Y)$ .

Squared loss has two motivations. First it corresponds to the Gaussian likelihood, making it a natural choice of loss function in the additive Gaussian noise setting. Another important motivation of squared loss is due to the fact that the mean vector  $\mu$  of  $Y$  minimizes the mean squared error  $\mathbb{E}\|Y - g\|_2^2$  over all  $g \in \mathbb{R}^n$  as long as  $\mathbb{E}\|Y\|_2^2 < \infty$ , which is clearly the case for the Poisson mean problem. Therefore, it is no surprise that squared loss is used by many authors when evaluating the performance of algorithms in the Poisson setting.

For Poisson-distributed random variables, deviance minimization is equivalent to maximum likelihood, thus deviance takes into account the nature of Poisson random variables. In the generalized linear models literature, deviance is proportional to the difference between the log likelihood function applied at the model’s output  $g(y)$  and the saturated model, and can be viewed as the Poisson counterpart of the *residual sum of squares* in Gaussian linear regression. In this work, we use deviance to evaluate model performance in a much more general framework than generalized linear models.

A minor caveat of using the deviance loss is that estimators  $g$  such that  $g_i(Y) = 0$  when  $\tilde{Y}_i > 0$ , such as the MLE  $g(Y) = Y$ , have diverging deviance error and risk. Intuitively, claiming  $\hat{\mu}_i = 0$  in Poisson estimation rules out the possibility of observing any nonzero value for  $\tilde{Y}_i$ . The deviance loss penalizes such an incorrect decision with infinite loss. Therefore, when using deviance loss, the estimator should not output  $\hat{\mu}_i = 0$ . In practice, we can use a shifted version of  $g$  by a small factor. For example,  $g_1(y) = g(y) + c$ , or  $g_2(y) = g(y)\mathbb{1}(g(y) > 0) + c\mathbb{1}(g(y) = 0)$  for a small constant  $c > 0$ . The choice of  $c$  is arbitrary and can have effects on the resulting expected loss, and appropriate values may vary from problem to problem.

The difference between deviance and squared loss functions can be remarkable in some scenarios. This is illustrated by a simple example: consider two pairs (1, 2) and (501, 502). The squared loss evaluated at both pairs is 1 since  $2 - 1 = 502 - 501$ . Deviance however is very different:  $\text{Dev}(1, 2) = 0.307$ , while  $\text{Dev}(501, 502) = 0.001$ . This is reasonable when we think about Poisson random variables, where a mean around 500 also has variance of 500, making an absolute difference of 1 a small variation when compared to this difference for a Poisson with mean (and variance) around 1. We provide a more detailed illustration of the similarity and difference of the two loss functions in an empirical bayes Poisson compound estimation problem, based on [Brown et al. \(2013\)](#), in [Appendix A](#). In this paper we illustrate our findings and present some specific results for both deviance and squared loss functions due to their natural importance. The issue of choice between these two loss functions probably depends on the specific context and is beyond the scope of this paper.

### 1.3 Unbiased estimators and related work

Risk and out-of-sample error estimation is a fundamental problem in statistics and machine learning and it has been vastly studied in the Gaussian setting. [Stein \(1981\)](#) proposed SURE, a well known unbiased risk estimator for weakly differentiable algorithms that is a direct consequence from Stein’s Lemma. Extensions of SURE were derived, such as [Tibshirani \(2015\)](#), who was able to accommodate some types of discontinuity in SURE, and [Tibshirani and Rosset \(2019\)](#), where the bias of SURE-tuned models was studied. Targeting a more general class of functions, [Breiman \(1992\)](#), [Ye \(1998\)](#), [Efron \(2004\)](#), and [Oliveira et al. \(2021\)](#) proposed new test error estimators without relying on the smoothness assumption of SURE; see detailed discussion in [Oliveira et al. \(2021\)](#).

[Hudson \(1978\)](#) presents a similar identity to Stein’s Lemma but generalized to exponential families. It has the form  $\mathbb{E}[(Y - \mu)g(Y)] = \mathbb{E}[a(Y)g'(Y)]$  for some  $a(Y) : \mathbb{R} \rightarrow \mathbb{R}$  and assumes that  $g$  is absolutely continuous. [Hwang \(1982\)](#) and [Ghosh et al. \(1983\)](#) used Hudson’s Lemma to improve on mean estimators for members of the discrete and continuous exponential families, respectively, and [Berger \(1980\)](#) uses Hudson’s Lemma to improve inadmissible estimators. Like Stein’s Lemma, [Hudson \(1978\)](#) uses this identity to construct unbiased error estimators under squared loss; however, because of  $a(\cdot)$ , the estimators target risk and/or error with respect to some transformation of the parameter  $\mu$ . For discrete distributions, instead of the derivative, the “change in  $Y$ ” is measured by  $g(Y - 1)$ , dropping the smoothness requirement. In particular, for the Poisson distribution,  $a(Y) = 1$ , leading to Lemma 1, PURE, and PUKLA ([Deledalle, 2017](#)).

**Lemma 1** (Hudson’s Lemma for the Poisson case). *Let  $Y_i \sim \text{Poisson}(\mu_i), i = 1, \dots, n$  and  $f : \mathbb{R}^n \rightarrow \mathbb{R}^n$  such that  $\mathbb{E}[|f_i(Y)|] < \infty \forall i \in [n]$ . Then,  $\mathbb{E}[\mu_i f_i(Y)] = \mathbb{E}[Y_i f_i(Y - e_i)]$ , where  $e_i \in \mathbb{R}^n$  is a vector whose  $i^{\text{th}}$  entry is 1 and the others are 0.*

PURE and PUKLA are risk estimators for squared and deviance loss that follow directly from Lemma 1:

$$\begin{aligned} \text{PURE} &= \|g(Y)\|_2^2 - 2\langle Y, g_-(Y) \rangle + \langle Y, Y - 1 \rangle \\ \text{PUKLA} &= \|g(Y)\|_1 - \langle Y, \log g_-(Y) \rangle, \end{aligned}$$

where  $\{g_-(Y)\}_i = g_i(Y - e_i)$ . While PURE is exactly unbiased for  $\text{Risk}^{(\text{Sqr})}$ , PUKLA is unbiased up to a constant for  $\text{Risk}^{(\text{Dev})}$ . PURE is widely used in the literature and in particular very often referenced in signal processing, such as [Luisier et al. \(2010\)](#), who introduces an algorithm for image restoration that targets Poisson noise by minimizing PURE, and [Le Montagner et al. \(2014\)](#), who proposes a risk estimator for mixed Gaussian-Poisson noise.

Pairing Lemma 1 with Efron’s Optimism Theorem for Bregman divergence loss ([Efron, 2004](#)), we obtain an unbiased estimator for out-of-sample loss in the Poisson case, described in Theorem 1. By phrasing it in terms of error instead of risk, we have an exactly unbiased error estimator for any Bregman divergence loss, and not up to a constant as PUKLA.

**Theorem 1.** *Let  $Y_i \sim \text{Poisson}(\mu_i), i = 1, \dots, n, \tilde{Y}$  and *i.i.d.* copy of  $Y, g : \mathbb{R}^n \rightarrow \mathbb{R}^n$ , and  $D_\phi$  be a Bregman divergence loss indexed by convex function  $\phi$  such that  $\mathbb{E}[|\phi'(g_i(Y))|] < \infty \forall i \in [n]$ . Then,*

$$\text{UE}(g) = \sum_{i=1}^n \phi(Y_i) - \phi(g_i(Y)) - 2\phi'(g_i(Y))Y_i + \phi'(g_i(Y))g_i(Y) + Y_i\phi'(g_i(Y - e_i)) \quad (2)$$

*is unbiased for Err, that is,  $\mathbb{E}[\text{UE}(g)] = \mathbb{E}[D_\phi(\tilde{Y}_i, g_i(Y))] = \text{Err}$ . The proof is in Appendix B.*

As an immediate consequence of Theorem 1, we have exactly unbiased estimators for out-of-sample error for both deviance and squared losses,

$$\begin{aligned} \text{UE}^{(\text{Sqr})}(Y) &= \|Y\|_2^2 - 2\langle Y, g_-(Y) \rangle + \|g(Y)\|_2^2 \\ \text{UE}^{(\text{Dev})}(Y) &= \sum_{i=1}^n 2Y_i \log Y_i - 2Y_i \log g_i(Y - e_i) + 2g_i(Y) - 2Y_i, \end{aligned}$$

For squared loss, we assume that  $\mathbb{E}[|g_i(Y)|] < \infty \forall i \in [n]$  and  $\mathbb{E}[\|g(Y)\|_2^2] < \infty$ , and for deviance loss,  $\mathbb{E}[|\log g_i(Y)|] < \infty \forall i \in [n]$ . The estimators PURE, PUKLA,  $\text{UE}^{(\text{Sqr})}(Y)$  and  $\text{UE}^{(\text{Dev})}(Y)$  can be used to

estimate an algorithm’s performance, tune hyperparameters, and perform model selection. However, they have one major downside: they are computationally inefficient, in particular when  $g$  is a complex algorithm. They require  $g$  to be run  $n + 1$  times in order to obtain the vector  $g_-(y)$ , which scales poorly with sample size, especially in modern applications that usually pair large scale datasets with high complexity algorithms. Our proposed coupled bootstrap estimator relies on a fixed number of refits of  $g$ , regardless of sample size.

Other approaches that are related to our problem of interest include AIC (Akaike, 1973), which limits the functional form of  $g$ , parametric bootstrap (Efron, 2004), which targets a conditional parameter instead of a marginal parameter, and adaptive model selection (Shen et al., 2004), that targets estimating generalized degrees of freedom, penalizing the log-likelihood, and performing model selection.

## 1.4 Paper organization

- In Section 2, we introduce CB, show that it is unbiased for an intuitive target and that this new target parameter converges to the original error.
- In Section 3, we show the limiting equivalence between the infinite bootstrap CB estimator and the unbiased estimator.
- In Section 4, we study the bias and variance of the CB estimator and how these quantities change with the CB parameters.
- In Section 5, we compare the CB estimator and the unbiased estimator performance in simulated scenarios and propose an adjustment to the unbiased estimator that minimizes computational cost but increases variability.
- In Section 6, we evaluate the performance of the CB estimator in the image denoising framework, an important use-case of our estimator. We find out that using deviance consistently results in more regularized models than squared loss.
- In Section 7, we describe Lindsey’s method for density estimation and use CB for the Poisson regression tuning step.
- In Section 8, we discuss our results and potential extensions of our framework, such as other distributions and loss functions, random versus fixed noise when tuning parameters, and the use of variance stabilizing transformations.

## 2 CB error estimator and basic properties

In this section, we present the CB estimator, show that it is unbiased for an intuitive parameter  $\text{Err}_p$ , and that  $\text{Err}_p$  is a continuous function of  $p$  for  $p \in [0, 1)$ , showing that our estimator is targeting a meaningful and well behaved parameter.

### 2.1 CB estimator

Following ideas from Oliveira et al. (2021), we propose a new estimator for the Bregman divergence test error of an arbitrary function  $g$  based on the coupled bootstrap (CB) approach when the response vector  $Y$  is Poisson with mean vector  $\mu$ . Our estimators are unbiased for intuitive and explicit targets: the error of  $g$  with respect to a Poisson random variable with shrunken mean vector  $(1 - p)\mu$ ,  $p \in (0, 1)$ ,

$$\text{Err}_p(g) = \mathbb{E}[D_\phi(\tilde{Y}_p, g(Y_p))], \quad \text{where } Y_{pi} \sim \text{Poisson}(\mu_i(1 - p)), \tilde{Y}_{pi} \text{ i.i.d. } Y_{pi}.$$

Different than the unbiased estimators, the CB estimator computational complexity is constant with respect to the sample size; the number of times algorithm  $g$  needs to be refitted is the number of CB paired samples,  $B$ , which in large scale applications is usually much smaller than sample size.

For a  $y \in \mathbb{N}_0^n$ , the notation  $\text{Binomial}(y, p)$  refers to a random vector in  $\mathbb{N}_0^n$  with independent  $\text{Binomial}(y_i, p)$  entries. The following lemma allows us to construct a pair of independent Poisson random vectors from  $Y$ .

The relationship presented in Lemma 2 is from Leiner et al. (2021), where the authors discuss data fission, a more general framework for splitting data into two parts such that together they recover the original data, but separately each part is not sufficient to reconstruct the data. The proof is deferred to Appendix D.

**Lemma 2.** *Let  $Y \sim \text{Poisson}(\mu)$  and  $(\omega|Y) \sim \text{Binomial}(Y, p)$ . Then,  $\omega \sim \text{Poisson}(\mu p)$  and  $Y - \omega \sim \text{Poisson}(\mu(1 - p))$  are independent.*

Given the data  $Y$ , a bootstrap sample size  $B$ , and perturbation level  $p \in (0, 1)$ , the CB error estimator is computed as follows.

$$\begin{aligned} (\omega^b|Y) &\sim \text{Binomial}(Y, p), \quad b = 1, \dots, B, \\ Y^{*b} &= Y - \omega^b, \quad Y^{\dagger b} = \frac{(1-p)}{p} \omega^b, \quad b = 1, \dots, B, \\ \text{CB}_p &= \sum_{b=1}^B \frac{1}{B} (D_\phi(Y^{\dagger b}, g(Y^{*b})) + \phi(Y^{*b}) - \phi(Y^{\dagger b})). \end{aligned} \quad (3)$$

For the two loss functions of interest, squared and deviance, Equation (3) can be reduced to

$$\begin{aligned} \text{CB}_p^{(\text{Sqr})} &= \sum_{b=1}^B \frac{1}{B} (\|Y^{\dagger b} - g(Y^{*b})\|_2^2 + \|Y^{*b}\|_2^2 - \|Y^{\dagger b}\|_2^2), \\ \text{CB}_p^{(\text{Dev})} &= 2 \sum_{b=1}^B \frac{1}{B} \sum_{i=1}^n (Y_i^{*b} \log Y_i^{*b} - Y_i^{\dagger b} \log g_i(Y^{*b}) + g_i(Y^{*b}) - Y_i^{\dagger b}). \end{aligned}$$

The idea is that, since  $(Y^{*b}, Y^{\dagger b})$  are two independent samples with the same mean  $\mu(1 - p)$ ,  $Y^{*b}$  acts as a training set for  $g$  and  $Y^{\dagger b}$  as a test set, evaluating how  $g$  performs when presented with a new independent sample. Although  $Y^\dagger$  is not Poisson distributed, it is a linear transformation of a Poisson, and  $g$  is trained on  $Y^{*b} \sim \text{Poisson}(\mu(1 - p))$ , which converges to  $Y \sim \text{Poisson}(\mu)$  as  $p \rightarrow 0$ . In the next section, we prove that  $\mathbb{E}[\text{CB}_p] = \text{Err}_p(g)$ , a strong unbiasedness property that does not require any assumptions on the function  $g$  other than integrability.

## 2.2 Unbiasedness for shrunken target

Our first main theorem states that the CB estimate is unbiased for a slightly shrunken target, namely  $\text{Err}_p$ , for *any* model  $g$  and any  $B$  under some mild integrability conditions.

**Theorem 2.** *Let  $Y, \omega$  be as defined in Lemma 2,  $Y^* = Y - \omega$  and  $Y^\dagger = \omega(1 - p)/p$ . Then, for any Bregman divergence  $D_\phi$ ,*

$$\mathbb{E}[D_\phi(\tilde{Y}^*, g(Y^*))] = \mathbb{E}[D_\phi(Y^\dagger, g(Y^*))] + \mathbb{E}[\phi(Y^*) - \phi(Y^\dagger)] \quad (4)$$

*provided all expectations are finite. Moreover,  $\mathbb{E}[\text{CB}_p^{(\text{Sqr})}] = \text{Err}_p^{(\text{Sqr})}(g)$  and  $\mathbb{E}[\text{CB}_p^{(\text{Dev})}] = \text{Err}_p^{(\text{Dev})}(g)$  assuming that  $\mathbb{E}[\|g(Y^*)\|_2^2] < \infty$  and  $\mathbb{E}[|Y_i^\dagger \log g_i(Y^*)|] < \infty$ , respectively. The proof is deferred to Appendix E.*

The main tool in the proof of Theorem 2 is Lemma 3 below, which states that for a given random vector  $U$ , if we are able to generate a vector  $W$  that is independent and has the same mean of  $U$ , we are able to unbiasedly estimate the test error of  $g$  applied to  $U$ . Note that the independence and same expectation requirement for  $W$  is very weak when compared to an i.i.d. assumption.

**Lemma 3.** *Let  $U, V, W \in \mathbb{R}^n$  be independent random vectors. For any  $g$ , and Bregman divergence  $D_\phi$ ,*

$$\mathbb{E}[D_\phi(V, g(U))] - \mathbb{E}[D_\phi(W, g(U))] = \mathbb{E}[\phi(V)] - \mathbb{E}[\phi(W)] + \langle \mathbb{E}[\nabla \phi(U)], \mathbb{E}[W] - \mathbb{E}[V] \rangle,$$

*provided all expectations are finite. In particular, if  $\mathbb{E}[V] = \mathbb{E}[W]$  and  $U, V$  are i.i.d., then*

$$\mathbb{E}[D_\phi(V, g(U))] = \mathbb{E}[D_\phi(W, g(U))] + \mathbb{E}[\phi(U)] - \mathbb{E}[\phi(W)].$$

**Remark 1.** The proof of Theorem 2 uses Lemma 3 with the correspondence  $U = Y^*$ ,  $V = \tilde{Y}^*$ , and  $W = Y^\dagger$ . Note that there are different ways to construct  $(U, V, W)$  that satisfy the conditions required in Lemma 3. For example, considering squared loss,

$$\begin{aligned}\text{CB}_{p,1}^{(\text{Sqr})} &= \|Y^\dagger - g(Y^*)\|_2^2 + \|Y^*\|_2^2 - \|Y^\dagger\|_2^2, \\ \text{CB}_{p,2}^{(\text{Sqr})} &= \|Y^\dagger - g(Y^*)\|_2^2 - \frac{(1-p)}{p} \langle Y^*, 1 \rangle - \langle Y^*, 1 \rangle, \\ \text{CB}_{p,3}^{(\text{Sqr})} &= \|Y^\dagger - g(Y^*)\|_2^2 - \frac{(1-p)}{p} \langle Y^\dagger, 1 \rangle - \langle Y^*, 1 \rangle\end{aligned}$$

are all unbiased for  $\text{Err}_p$ . However, they have different variances, and our choice of  $\text{CB}_p^{(\text{Sqr})} = \text{CB}_{p,1}^{(\text{Sqr})}$  is due to it having the smallest variance among the three when  $p$  is small, which is discussed in Section 4.

We have shown that the coupled bootstrap estimator is unbiased for the shrunken target  $\text{Err}_p(g)$ , considering both loss functions. Now, we motivate the use of this new target by investigating if the shrunken target is close to the original  $\text{Err}(g)$ . In fact, if  $g$  satisfies a moment condition, then the map  $p \mapsto \text{Err}_p(g)$  is continuous and has  $k$  continuous derivatives on the interval  $p \in [0, 1)$ . This is summarized in the following proposition, whose proof is deferred to Appendix F.

**Proposition 1.** For  $p \in [0, 1)$ , define  $Y_p$  a  $n$ -dimensional vector of independent Poisson random variables where the  $i^{\text{th}}$  entry has mean  $\mu_i(1-p)$  and  $\tilde{Y}_p$  is an i.i.d. copy of  $Y_p$ . Let  $f : \mathbb{N}_0^n \times \mathbb{N}_0^n \mapsto \mathbb{R}^+$  and for an integer  $k \geq 0$ , assume  $\mathbb{E}[f(Y_0, \tilde{Y}_0) \langle \tilde{Y}_0 + Y_0, \mathbf{1}_n \rangle^k] < \infty$ . Then, the map  $p \mapsto \mathbb{E}[f(\tilde{Y}_p, Y_p)]$  has  $k$  continuous derivatives on  $[0, 1)$ .

**Remark 2.** By assuming only that the out of sample error is finite ( $\text{Err} < \infty$ ), we have  $\lim_{p \rightarrow 0} \text{Err}_p(g) = \text{Err}(g)$ . This means that the parameter targeted by the CB estimator converges to the original parameter of interest as  $p$  decreases for all  $g$  that have a finite out-of-sample error.

### 3 Relationship between limiting CB and unbiased estimator

In this section we study the relationship between the limiting CB estimators as  $p \rightarrow 0$  and the exactly unbiased estimators from Section 1.3. We consider the infinite bootstrap estimator  $\text{CB}_p^\infty(g)$ , which assumes an infinite number of bootstrap samples. By the Law of Large numbers, this estimator is equivalent to taking the expectation over  $\omega$ ,

$$\text{CB}_p^\infty(g) = \mathbb{E}[\text{CB}_p(g)|Y],$$

where  $\text{CB}_p(g)$  considers  $B = 1$ . Note that, although incomputable in practice,  $\text{CB}_p^\infty(g)$  is still a function of the data  $Y$  and therefore an estimator and a random variable.

**Theorem 3.** Let  $D_\phi$  be a Bregman divergence loss and  $g_i$  be such that (a)  $\mathbb{E}|\phi(g_i(Y))| < \infty$ ,  $\mathbb{E}|\phi'(g_i(Y))| < \infty$  for all  $i$ ; and (b) both  $\phi(g_i(\cdot))$  and  $\phi'(g_i(\cdot))$  can be extended to  $(\mathbb{N}_0 \cup \{-1\})^n$  such that the functions take value 0 if the  $i$ th coordinate of the input is  $-1$ . Then,

$$\lim_{p \rightarrow 0} \mathbb{E}[\text{CB}_p(g)|Y] = \text{UE}(Y)$$

almost surely, where  $\text{UE}(Y)$  is the estimator defined in Equation (2). The proof is deferred to Appendix F.

Theorem 3 shows that when the shrinking factor  $p$  goes to 0 and  $B \rightarrow \infty$ , the CB estimators fully recover the exactly unbiased estimators derived from Hudson's Lemma, for every sampled vector  $y$ . An immediate consequence of this result is that  $\text{CB}_p^\infty(g)$  is asymptotically unbiased for the test error of the unshrunk variable of interest

$$\mathbb{E} \left[ \lim_{p \rightarrow 0} \mathbb{E}[\text{CB}_p(g)|Y] \right] = \lim_{p \rightarrow 0} \mathbb{E}[\mathbb{E}[\text{CB}_p(g)|Y]] = \lim_{p \rightarrow 0} \text{Err}_p = \text{Err}.$$

Also, note that Theorem 3 does not require any extra assumptions on  $g$  that is not already required by Hudson's Lemma. In particular, for squared loss,  $\lim_{p \rightarrow 0} \mathbb{E}[\text{CB}_p^{(\text{Sqr})}(g)|Y] = \text{UE}^{(\text{Sqr})}(Y)$  as long as  $g_i$  and  $g_i^2$  have finite expectation for  $i \in [n]$ , and for deviance loss  $\lim_{p \rightarrow 0} \mathbb{E}[\text{CB}_p(g)|Y] = \text{UE}^{(\text{Dev})}(Y)$  as long as  $g_i$  and  $\log g_i$  have finite expectation for  $i \in [n]$ .

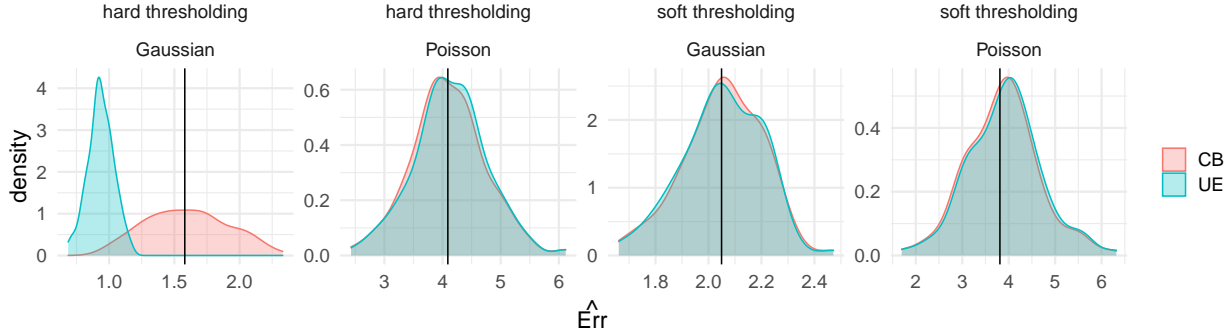


Figure 1: Density of  $\mathbb{E}[\text{CB}|Y]$  and  $\text{UE}(Y)$  for Gaussian and Poisson settings, considering a hard-thresholding style estimator and a soft-thresholding style estimator. For the Gaussian case, SURE is used as  $\text{UE}(Y)$ . The black vertical line is the true  $\text{Err}$ .

**Remark 3.** The fact that CB fully recovers UE under specific conditions corroborates with the quality and construction of our estimator. It shows a better understanding of what we are proposing, even if the limiting estimator is not computable in practice (since it relies on infinite bootstrap samples and  $p \rightarrow 0$ ).

**Remark 4.** In the Gaussian case, the infinite CB estimator recovers SURE (Stein, 1981) as the noise level goes to 0, being unbiased under a weak differentiability assumption (Oliveira et al., 2021). Theorem 3, which is tailored for the Poisson setting, does not require any type of smoothness assumption on  $g$  to recover UE. To illustrate this difference, we run a short simulation considering squared loss. Set  $n = 30$ , the relative perturbation of  $\text{Var}[Y^*]$  with respect to  $\text{Var}[Y]$  to be 0.01,  $\mu_i = 2$ ,  $i = 1, \dots, 30$ , and consider two functions  $g$ : a weakly differentiable soft thresholding style estimator  $g(y) = 0.5\mathbb{1}(y < 2) + (y + 0.5 - 2)\mathbb{1}(y \geq 2)$  and a hard thresholding style  $g(y) = 0.5\mathbb{1}(y < 2) + y\mathbb{1}(y \geq 2)$ . We generate 100 vectors  $Y$ , both Gaussian (with  $\sigma^2 = 0.3$ ) and Poisson, and approximate  $\mathbb{E}[\text{CB}|Y]$  with  $10^5$  samples of  $\omega$ . We compare them to UE (or SURE in the Gaussian setting). For the nondifferentiable  $g$  and Gaussian noise, we use the a.e. derivative to compute the divergence required by SURE. Results are in Figure 1. Each plot shows the true error (black vertical line) and the empirical density of CB (red) and of the unbiased estimator (blue). While smoothness is not a problem for CB in the Poisson setting, it clearly makes SURE biased, which is consistent with the theoretical findings.

## 4 Bias and variance

In this section, we analyze the bias-variance decomposition of the CB estimator when targeting the averaged original error  $\text{Err}(g)/n$  for fixed  $p$  and  $B$ . We chose to present this section in terms of the averaged error to better understand how our estimator performs as  $n$  varies. The bias measures how far  $\text{Err}_p$  is from  $\text{Err}$ . We divide the variance in two components: the reducible variance, which can be controlled by increasing  $B$  and is the expectation of the conditional variance, and the irreducible variance, intrinsic to the problem and the variability of  $g(Y)$  and is the variance of  $\text{CB}_p^\infty(g)$ . This decomposition is given by

$$\mathbb{E} \left[ \frac{\text{CB}_p(g) - \text{Err}(g)}{n} \right]^2 = \underbrace{\left[ \frac{\text{Err}(g) - \text{Err}_p(g)}{n} \right]^2}_{\text{Bias}^2(\text{CB}_p(g))} + \underbrace{\mathbb{E} \left[ \text{Var} \left( \frac{\text{CB}_p(g)}{n} \mid Y \right) \right]}_{\text{RVar}(\text{CB}_p(g))} + \underbrace{\text{Var} \left( \mathbb{E} \left[ \frac{\text{CB}_p(g)}{n} \mid Y \right] \right)}_{\text{IVar}(\text{CB}_p(g))},$$

where we used the unbiasedness of CB to a shrunken target and the Law of Total Variance. In propositions 2, 3, and 4, we analyze how each of these terms depend on the two user-chosen parameters  $p$  and  $B$ , with a focus on small  $p$ . The proofs of these propositions are deferred to Appendix H.

We start with the bias term. Proposition 2 provides an exact expression for bias and an inequality that shows that for small  $p$ , the bias decreases linearly with  $p$ . The bias magnitude also increases with the variability of the loss function applied to the random variable of interest: the more variable, the larger the difference between  $\text{Err}$  and  $\text{Err}_p$ .

Table 1: Minimum value for  $B$  considering different combinations of  $\mu$  and  $p$  when  $n = 1$ .

$p = 0.1$	$\mu$	0.5	1	5	10	30	100
	$B$	5	10	50	100	900	10000
$\mu = 5$	$p$	0.001	0.005	0.01	0.1	0.3	0.5
	$B$	5000	1000	500	50	25	25

**Proposition 2** (Bias). *For a Bregman divergence loss function  $D_\phi(\cdot, \cdot)$ , assume  $\mathbb{E}[D_\phi(\tilde{Y}_i, g_i(Y))\langle Y_i + \tilde{Y}_i, \mathbf{1}_n \rangle] < \infty$ . Let  $p \in [0, 1)$ . Then,*

$$\begin{aligned} \text{Bias}(\text{CB}_p(g)) &= \frac{1}{n} |\text{Err} - \text{Err}_p| \\ &= \frac{1}{n} \left| \int_0^p \frac{1}{\sqrt{1-t}} \text{Corr}[D_\phi(\tilde{Y}_t, g(Y_t)), \langle \tilde{Y}_t + Y_t, \mathbf{1}_n \rangle] \sqrt{\text{Var}[D_\phi(\tilde{Y}_t, g(Y_t))]} dt \right| \left( 2 \sum_{i=1}^n \mu_i \right)^{1/2}. \end{aligned}$$

Moreover, for small  $p$ ,

$$\text{Bias}(\text{CB}_p(g)) \leq \frac{p}{n} \sqrt{\text{Var}[D_\phi(\tilde{Y}, g(Y))]} \left( 2 \sum_{i=1}^n \mu_i \right)^{1/2} + O(p^{3/2}/n).$$

Now we analyze the irreducible variance. The irreducible variance term represents the variability due to the sampling process of  $Y$ . Because this term is the variability of the infinite bootstrap  $\text{CB}^\infty$ , in Proposition 3 we are able to show that for infinitesimal  $p$ , the added randomness from generating  $\omega$  does not affect  $\text{IVar}(\text{CB}_p(g))$ .

**Proposition 3** (Irreducible variance). *Let  $\tilde{g} : \mathbb{R}^n \rightarrow \mathbb{R}^n$  such that  $\tilde{g}(y) = \max_{x \in \mathcal{Y}} g(x)$ , where  $\mathcal{Y} = \{z \in \mathbb{N}_0^n : 0 \leq z_i \leq y_i \forall i \in [n]\}$ . Assume that  $\mathbb{E}[\langle \phi'(\tilde{g}(Y)), Y \rangle^2] < \infty$ . Then,*

$$\lim_{p \rightarrow 0} \text{IVar}(\text{CB}_p(g)) = \lim_{p \rightarrow 0} \text{Var}[\mathbb{E}[\text{CB}_p/n|Y]] \leq \frac{2}{n^2} \text{Var}[D_\phi(Y, g(Y)) + \langle Y, \phi'(g(Y)) \rangle] + \frac{2}{n^2} \mathbb{E}[\langle \phi'(\tilde{g}(Y)), Y \rangle^2].$$

Finally, we analyze the reducible variance. This term consists of the variability due to the noise-adding construction of CB and its dependency on  $p$  and  $B$ . Proposition 4 shows that this term can be controlled by increasing  $B$ .

**Proposition 4** (Reducible variance). *Let  $\mathbb{E}[\phi'(g_i(Y^*))^2] < \infty$  for all  $i \in [n]$ . Then,*

$$\begin{aligned} \mathbb{E}[\text{Var}[\text{CB}_p/n|Y]] &\leq \frac{2}{Bn^2} \text{Var}[D_\phi(Y, g(Y)) + \langle Y, \phi'(g(Y)) \rangle] + \frac{2}{Bn^2} O(p) + \frac{2}{Bn^2 p} \sum_{i=1}^n \mu_i \mathbb{E}[\phi'(g_i(Y^*))^2] \\ &\quad + \frac{2}{Bn^2} \sum_{i=1}^n \mu_i^2 (\text{Var}[\phi'(g_i(Y^*))] + O(p)). \end{aligned}$$

But how large should  $B$  be? There are two quantities that  $B$  should balance out:  $p$  and the signal size. Ideally, one wants  $B > \max\{\frac{1}{p} \sum_{i=1}^n \mu_i, \sum_{i=1}^n \mu_i^2\}$ . Table 1 shows the minimum value for  $B$  in some settings, considering  $n = 1$ . Note that for a fixed  $\mu$ ,  $B$  does not get too high considering reasonable practical values of  $p$ , such as 0.1. However, for a fixed  $p$ , a high  $\mu$  increases the reducible variance term a lot, requiring a much larger  $B$ . In practice, it is hard to have an idea of the  $\mu_i$ 's. Since high  $\mu_i$ 's lead to high observed  $y$ , our suggestion is to increase  $B$  when a great proportion of high  $y$ 's is in the sample.

**Remark 5.** To better understand the reducible variance term and the quality of the bound, we run the following simulation: set  $n = 100$ ,  $p = 0.1$ , and  $g(y) = 0.8y + 0.1$ . We vary two quantities:  $B$ , from 30 to 1000, and  $\mu$ , from 0.1 to 50. Note that all 100 entries of  $Y$  have the same mean  $\mu$ . For each  $(B, \mu)$  we approximate the reducible variance and the upper bound via MC, where we use 10000 samples of  $Y$  and for each  $Y$ , 10000 samples of  $\omega|Y$ . Results are in Figure 2, where we present the logarithm of the reducible variance term. The two panels look very similar for both loss functions, indicating that the relationship between  $B$ ,  $p$ , and  $\mu$  was correctly captured by Proposition 4.

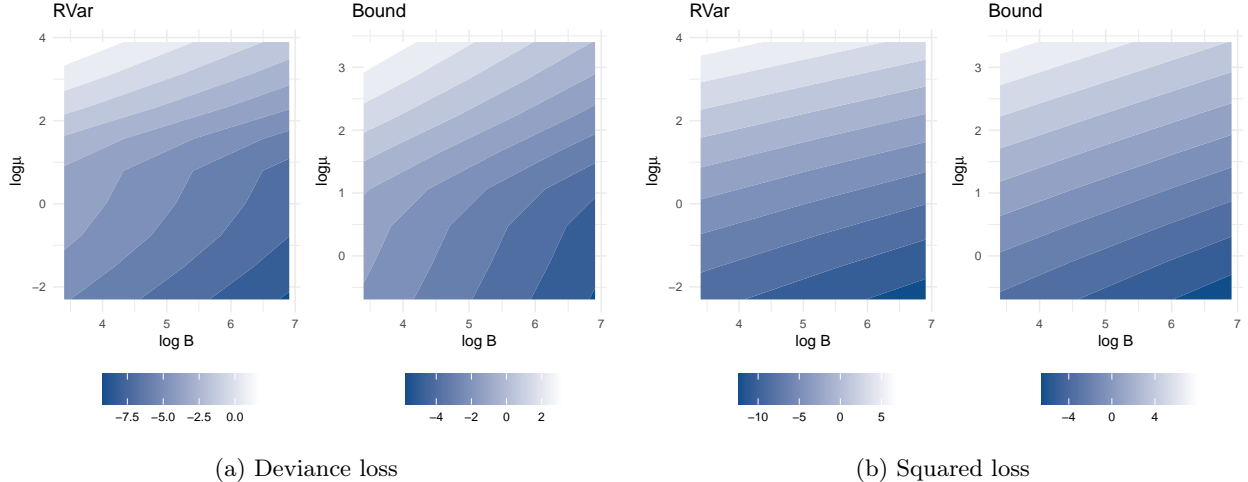


Figure 2: Curve levels of logarithm of reducible variance and logarithm of the proposed bound, as a function of  $\log B$  and  $\log \mu$ . The left plot shows reducible variance and its bound for deviance loss, while the plot on the right considers squared loss.

## 5 Experiments

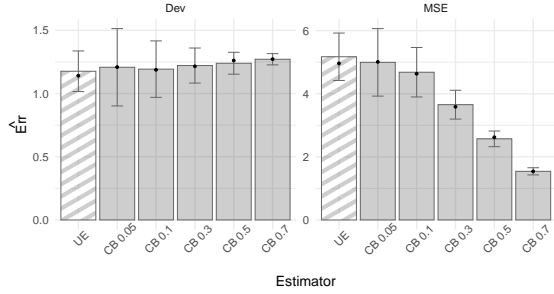
In this section, we run two simulation sets. First, we compare the performance of CB and UE in different model settings, fitting functions  $g$ , and perturbation level  $p$ . We find that the overall performance of CB is comparable to that of UE in most cases, but CB has much smaller variance than UE when the estimator  $g$  is unstable. Second, we fix the model, fitting function, but focus on the performance of CB and UE under equal computational cost controlled by  $(n, B)$ . In general, CB seems to be a better choice unless the true mean is very high.

### 5.1 Comparing CB and the full version of UE

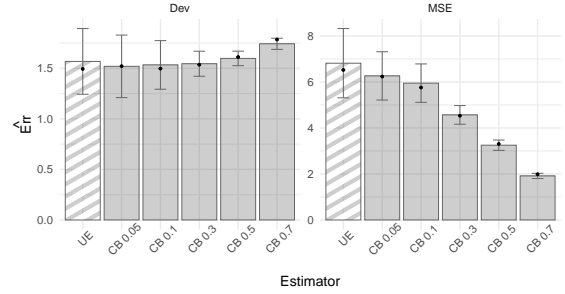
For CB, we vary  $p = 0.05, 0.1, 0.3, 0.5, 0.7$ . Throughout, we set  $n = 100$ ,  $B = 100$ , and 100 replications are used to approximate the expected values. Note that in this low sample size scenario, the computational cost between the two estimators is the same.

First, we consider the “many Poisson means” problem where the first 10 means are 10 and the others are 0.5. Figure 3c shows the behavior of the error estimators when  $g$  is the first step improvement on EB as described in Section 1.2 with fixed  $h = 0.85$ . Then, we consider a Poisson regression setting, where  $Y \sim \text{Poisson}(e^{X\beta})$ ,  $\beta_1, \dots, \beta_{10} = 0.05$ , and  $X \sim N_{10}((3, \dots, 3), I)$  is generated once and fixed throughout the simulations, resulting in  $\text{SNR} \approx 2$ . The resulting means range from 2.75 to 6.46 and are symmetrically distributed. The considered  $g$ ’s are Poisson regression (Figure 3a) and regression trees (Figure 3b). The final set-up consists of a highly unstable  $g$ , cross-validated lasso Poisson regression (Figure 3d). In this case, at each replication, an  $\ell_1$ -penalized Poisson regression is fitted where the tuning parameter is selected through 5-fold cross-validation. For this experiment, we increase the number of features to 200, resulting in a high-dimensional problem. As in the previous simulation, we keep SNR at 2, and have set  $X \sim N_p((0, \dots, 0), 1.5 \times I)$  and  $\beta \in \mathbb{R}^p$ ,  $\beta_i = 0.13 \forall i \in [p]$ . The means of the 100 Poisson random variables are between 0.002 and 111.2, heavily right skewed. In each panel of Figure 3, bar heights are the averaged estimators over 100 replications and error bars are  $\pm$  one standard error. Black points are the approximation over 100 MC samples of test error considering  $p = 0, 0.05, 0.1, 0.3, 0.5, 0.7$ . The x-axis indicates the estimator, starting from UE (striped bars), which estimates Err, and followed by CB with increasing  $p$  (gray bars).

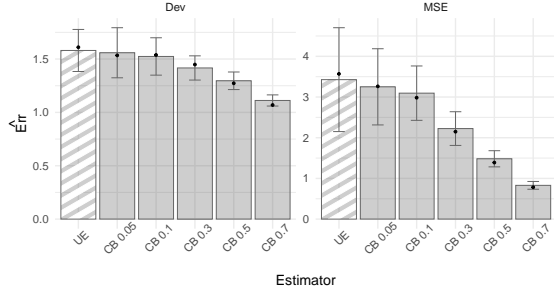
As expected, all estimators are unbiased for their target parameters. In all settings, the variability of CB decreases as  $p$  increases, which is expected since higher  $p$  leads to a  $Y^*$  with lower variance. As  $p$  varies, deviance error varies less than squared error. When comparing the variability of the UE and CB estimators, in figures 3c and 3b, UE’s variability is similar to  $\text{CB}_{p=0.05}$ , while in Figure 3a UE has lower variance. Regarding



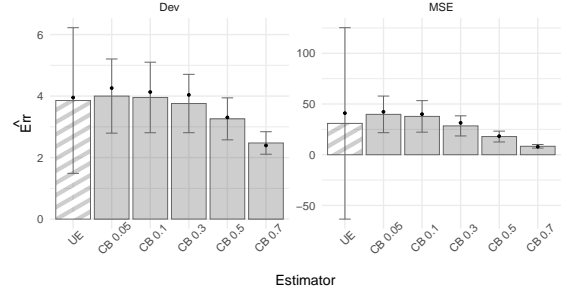
(a) Supervised learning,  $g =$  Poisson regression



(b) Supervised learning,  $g =$  regression tree



(c) Many Poisson means,  $g =$  EB step-1 improvement



(d) High dim. supervised learning,  $g =$  5-fold CV lasso

Figure 3: Comparison of test error estimators considering squared and deviance loss functions. Bar heights represent the average value of the estimator across 100 replications, and the error bars are the average  $\pm$  one standard error. Results for the Unbiased Estimator are shown by the bars with stripes, while results for CB and different values of  $p$  are shown by the grey bars. Each plot (a)-(d) consists of a different simulated setting, and in all settings we show results for deviance and squared loss functions.

squared loss, UE has lower variance than  $CB_{p=0.05}$  when  $g$  is the identity function and it has higher variance than  $CB_{p=0.05}$  when  $g$  is the step-1 improvement on EB. Figure 3d shows a scenario with unstable  $g$ , leading to UE having high variability. This does not happen to CB thanks to averaging the estimated errors across different noise replications, acting as bagging and diluting discrepant error values. This phenomena also happens with CB in the Gaussian setting, which is discussed in Oliveira et al. (2021).

## 5.2 Equating computational cost: the sampling summands UE vs CB

The UE estimator relies on  $n + 1$  refits of  $g$ , making it computationally expensive for large sample problems. In contrast, the number of refits required by CB is constant  $B$ . We consider a modified version of UE based on a *sampling summands* approach, so that it can have the same computational cost as CB. The idea is to replace the average over  $n + 1$  refits by averaging over the refits at  $B_{ss}$  randomly subsampled values. The resulting estimate, called  $UE_{ss}$ ,  $B_{ss} + 1$  fits of  $g$  and is unbiased for  $Err$  by construction. If  $B_{ss} = B$  then  $UE_{ss}$  and CB have roughly the same computational cost.

For the simulation that follows, let  $g(y) = 0.8y + 0.2\bar{y} + 0.01\mathbb{1}(\bar{y} = 0)$ ,  $Y_i \sim \text{Pois}(\mu)$ ,  $i = 1, \dots, n$ ,  $\mu \in \mathbb{R}^1$ . There are 5 parameters that affect variability:  $n$ ,  $\mu$ ,  $B$ ,  $B_{ss}$ , and  $p$ . To focus on the effect of  $n$  and  $B$ , we choose  $p = \min\{0.1, \sum_{i=1}^n \mu_i / \sum_{i=1}^n \mu_i^2\}$  so that  $p$  is not too large and is in the leading term of the reducible variance upper bound. We set  $B_{ss} = B = \max\{\frac{1}{p} \sum_{i=1}^n \mu_i, 100\}$  so that the reducible variance upper bound is at most a constant. We then vary two quantities,  $n$  from  $10^3$  to  $10^5$  and  $\mu$  from 0.5 to 30. Note that  $n$  is always greater or equal to  $B$ .

The level curves of the variances as functions of  $n$  and  $\mu$  are in Figure 4. For both loss functions, the variance of CB increases as  $\mu$  increases and it decreases as  $n$  increases. CB's highest variance is observed in the upper left corner, when the mean is highest and sample size is lowest. Considering deviance loss,  $UE_{ss}$  overall has higher variance than CB but in the upper left corner; however, in this low sample size scenario,

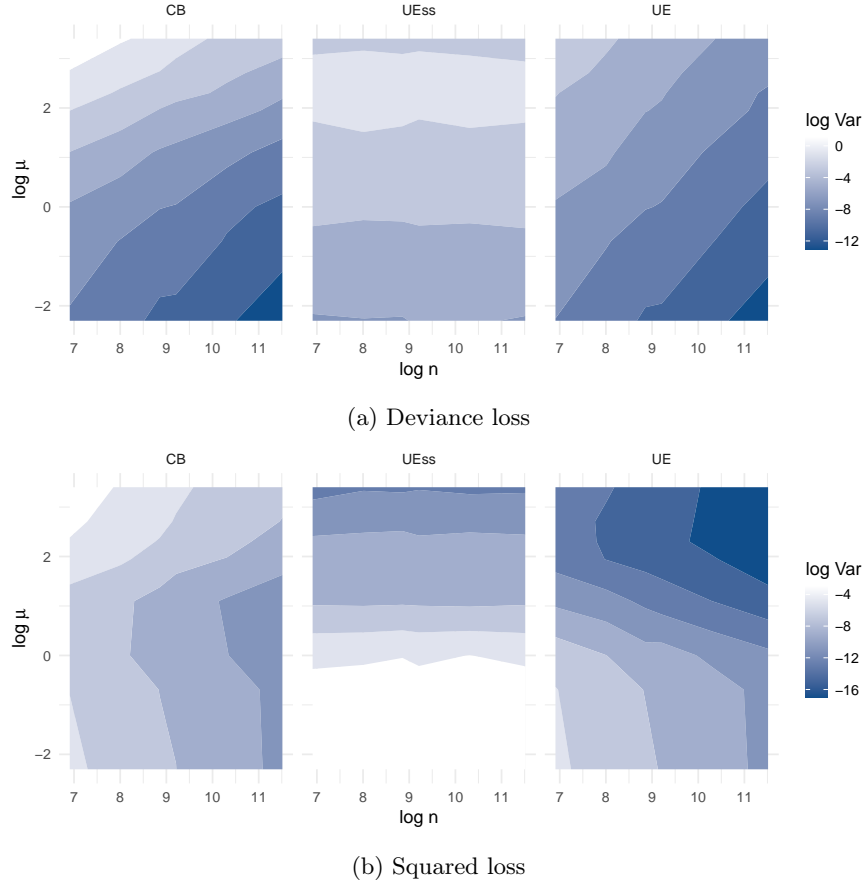


Figure 4: Curve levels of the logarithm of the variance of CB,  $UE_{ss}$ , and UE with varying  $\log n$  and  $\log \mu$ .

UE is viable and therefore a better choice. Under squared loss, CB has lower variance than  $UE_{ss}$  but on high  $\mu$  settings.

Overall, UE has the lowest variance. When compared to CB, we expect UE to have lower variance since while CB trains and tests  $g$  on  $Y^\dagger$  and  $Y^*$ , which by construction can be very different in magnitude, UE (roughly) trains and tests  $g$  on  $Y - 1$  and  $Y$ , which are always only one unit apart. The exception to this logic is when  $g$  is highly unstable and the bagging effect from CB controls the increased variability due to  $g$ , as illustrated by Figure 3d from Section 5.1. By construction, UE is expected to have lower variance than  $UE_{ss}$ . The difference between squared and deviance loss results are due to the difference in the loss functions functional form.

## 6 Application 1: Poisson image denoising

Poisson noise, also called shot noise or photon noise, is *signal dependent*. It is usually imperceptible in common images, but it can dominate scientific and low-light images such as microscopy and astronomical photography. It is caused by the discrete nature of electric charges and light particles – on each pixel of an image, for example, we count the number of independent photons arrival, which is a Poisson distributed random variable. While Gaussian noise is independent of the unknown signal and can be controlled (or reduced) with better equipment and technique, there is no improvement in equipment that controls Poisson noise.

The Poisson denoising problem has been widely studied, mostly in the signal processing literature. An intuitive approach is penalized maximum likelihood. [Lingens et al. \(2009\)](#) compares the use of three different penalizations for sparse signals. Poisson compressed sensing is a generalization of the Poisson

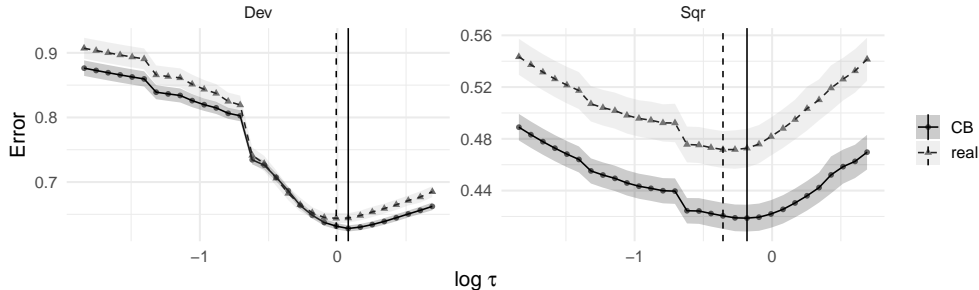


Figure 5: Real and estimated error considering different values of  $\tau$ . Average  $\pm$  standard errors across 30 replications.

denoising problem (Harmany et al., 2009; Luisier et al., 2010; Raginsky et al., 2010; Harmany et al., 2012; Salmon et al., 2014; Cao and Xie, 2016). Many authors propose transforming the data followed by Gaussian denoising (Dupé et al., 2009; Makitalo and Foi, 2009; Azzari and Foi, 2016; Zhang et al., 2019). In general, these works do not present a discussion on how hyperparameter tuning should be performed in practice, and model quality and performance is evaluated based on the true image (i.e., in-sample prediction error). Moreover, the authors acknowledge the importance of tailoring denoising methods to a Poisson setting, many using deviance as the loss function for model training; however, squared loss is commonly used to evaluate the performance.

We consider the following image denoising framework from Harmany et al. (2012). Let  $f^* \in \mathbb{R}_+^m$  sparse or compressible in some basis be the image of interest of size  $m$  and  $A \in \mathbb{R}^{N \times m}$  projects the  $f^*$  onto a  $N$ -dimensional space. Observed data consists of  $y \in \mathbb{N}_0^m$  where  $y \sim \text{Pois}(Af^*)$ . The estimator  $\hat{f}$  is given by the solution of the following optimization problem:

$$\hat{f} = \arg \min_{f \geq 0} \sum_{j=1}^N [(Af)_j + \beta - y_j \log((Af)_j + \beta)] + \tau \|f\|_{TV}, \quad (5)$$

where  $\beta$  is a small positive constant to avoid the singularity  $f = 0$  and  $\|f\|_{TV}$  is the TV seminorm defined as

$$\|f\|_{TV} \triangleq \sum_{k=1}^{\sqrt{n}-1} \sum_{l=1}^{\sqrt{n}} |f_{k,l} - f_{k+1,l}| + \sum_{k=1}^{\sqrt{n}} \sum_{l=1}^{\sqrt{n}-1} |f_{k,l} - f_{k,l+1}|. \quad (6)$$

Note that the formulation is equivalent to finding the optimal  $\hat{f}$  that minimizes the negative Poisson likelihood, equivalent to minimizing deviance, plus a penalty term that increases as the difference between neighboring pixels increases. The authors propose an algorithm tailored to solve this minimization problem, which we use as the fitting function  $g$ .

For our simulations, set  $A = I$ . This reduces the optimization problem described in Equation (5) to a standard Poisson denoising problem. We apply this denoising algorithm to the well-known phantom artificial image, which has  $128 \times 128$  pixels. For CB, we use  $B = 50$  and  $p = 0.1$ . The unbiased estimator is not considered in these experiments due to its computational cost.

First, we approximate the true out-of-sample error and expected CB error, considering both squared and deviance loss functions. 30 values for  $\tau$  are considered, from 0.15 to 2. To approximate the true error and the mean and variance of the CB estimator, we averaged results from 30 simulated noisy images. Figure 5 shows the average error and standard errors for different values of  $\tau$  and different loss functions. Deviance is minimized on higher values of  $\tau$  than squared loss, resulting in a more regularized image. For both loss functions, CB selected a higher  $\tau$  than real error. Different results are not surprising since CB estimates  $\text{Err}_{0.1}$  instead of  $\text{Err}_0$ . Figure 6 shows a histogram of the difference between optimal  $\tau$  selected via deviance and via squared loss over the 30 replications; note that the observed difference was always positive and far from 0, showing that deviance consistently leads to more regularization in this setting than squared loss.

To visualize the result of the tuned denoiser, we now consider only one noisy image and perform tuning. Figure 7 shows the estimated error curves using CB. As expected, squared loss selected in a smaller value of

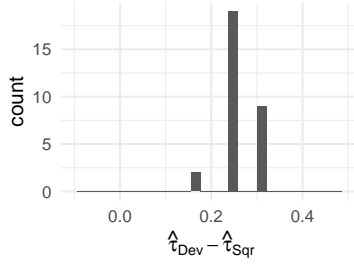


Figure 6: Histogram of the differences between optimal lambda selected via deviance minimization and via squared loss minimization, over 30 replications.

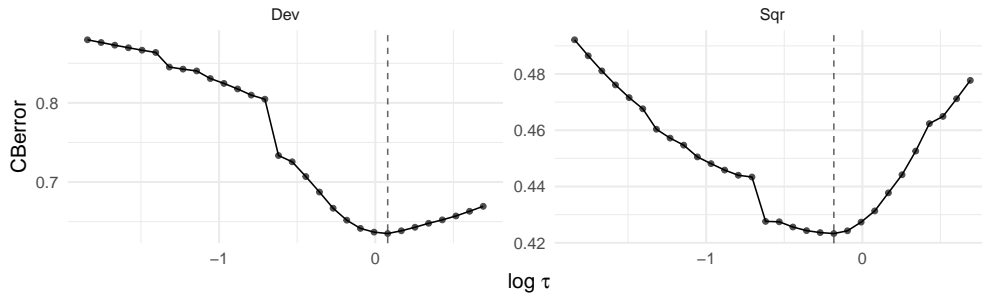


Figure 7: Estimated error via CB considering different values of  $\tau$  (black points and continuous black line). Dashed grey line is the  $\hat{\tau}$  that minimizes the estimated error.

$\tau$  than deviance. Moreover, in the neighborhood of the selected  $\tau$ , there is a steeper increase in error as  $\tau$  increases for squared loss when compared to the behavior of the error curve when  $\tau$  decreases. The opposite happens to deviance; the estimated error curve around the selected  $\tau$  grows more quickly for lower  $\tau$ 's than higher values of  $\tau$ . The original signal, noised image, denoised via deviance minimization, and denoised via squared loss minimization are in Figure 8. Visually, the tuning parameter value that minimized deviance produced an image that looks more similar to the original signal than the one that minimized squared loss.

## 7 Application 2: Density estimation via Lindsey's method

Another natural application of our CB estimator for Poisson variables is density estimation via Lindsey's method (Lindsey, 1974; Lindsey and Mersch, 1992; Efron and Tibshirani, 1996; Gao and Hastie, 2021). The

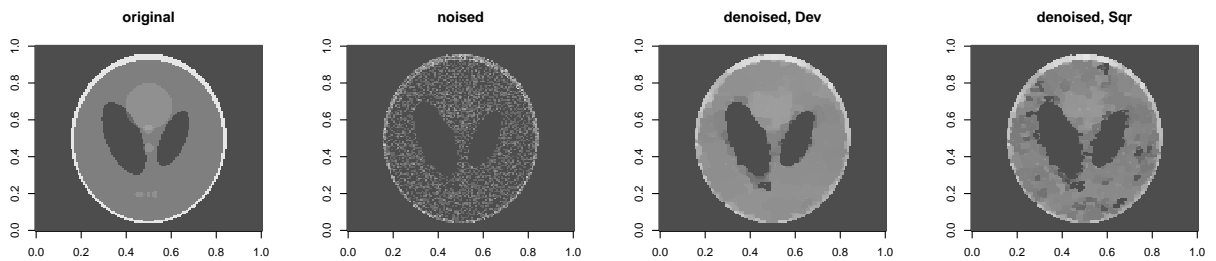


Figure 8: Results for the phantom image denoising example: original image ( $f$ ), noised image ( $y$ ), denoised image by minimizing squared CB error estimate, and denoised image by minimizing deviance CB error estimate.

idea behind Lindsey’s method is to discretize the space in bins and model the counts as a multinomial distribution; the estimated probabilities of the bins is the estimated density. The multinomial estimation process is phrased as a Poisson regression problem.

Let  $y_1, \dots, y_n$  be a sample from  $Y \sim f(y)$  and denote the sample space by  $\mathcal{Y}$ . Lindsey’s method first discretizes  $\mathcal{Y}$  into  $K$  disjoint bins  $\mathcal{Y}_k, k \in [K]$ , where  $\cup_{k=1}^K \mathcal{Y}_k = \mathcal{Y}$ . Define a new set of random variables  $s_k = \#\{y_i \in \mathcal{Y}_k, i = 1, \dots, n\}, k = 1, \dots, K$ . We can approximate the density  $f$  by considering the multinomial model  $(s_1, \dots, s_K) \sim \text{Multinomial}_K(n, (\pi_1, \dots, \pi_K))$ , where  $\pi_k = \int_{\mathcal{Y}_k} f(y)dy$ . Now, assume that  $n$  is a realization of the random variable  $s_+ \sim \text{Pois}(\gamma)$ . Then,

$$(s_1, \dots, s_K) | s_+ = n \sim \text{Multinomial}_K(n, (\pi_1, \dots, \pi_K)) \quad (7)$$

and for  $k \in 1, \dots, K$

$$s_k \sim \text{Pois}(\gamma\pi_k). \quad (8)$$

For a point  $y_k$  in bin  $\mathcal{Y}_k$  (e.g., the centroid of  $\mathcal{Y}_k$ ), we can approximate its pmf as  $F(y_k; \theta) = \exp\{\sum_{j=1}^p t_j(y_k)\theta_j + c(\theta) + d_2(y_k)\}$ . Then, by replacing  $c(\theta)$  by an unknown parameter  $\theta_0$ , and considering  $f_0(y_k) = \exp\{d_2(y_k)\}$  a carrier density, we can parametrize model (8) as

$$\gamma\pi_k(\theta) = f_0(y_k) \exp\left\{\sum_{j=1}^p t_j(y_k)\theta_j + \theta_0\right\}, \quad (9)$$

which can be fitted by a Poisson regression with  $K$  observations where the features are the sufficient statistics and the response variable is  $s_k$ . For a known parametric distribution (and using its sufficient statistics as  $t_j(y_k)$ ), this results in approximately the usual maximum likelihood estimator, the only difference being due the discretization process. However, this approach allows for a lot more flexibility, both through the carrier density and through the sufficient statistics, that can be complex basis functions with or without added penalization. In the case where a penalty term is added to the Poisson regression to control the basis functions coefficients, we tune the penalization using CB.

**Remark 6.** [Brown et al. \(2009\)](#) proposed the root-unroot method for density estimation, which is very similar to Lindsey’s method. It consists of the same discretization process, however, before the regression step, the data is transformed with the variance stabilizing transformation  $f(s_k) = \sqrt{\frac{K}{n}(s_k + 1/4)}$  (root step) and a gaussian regression is applied. We discuss variance stabilizing transformations and how the CB estimator can be used in this setting in Section 8.

In our implementation, we use a constant carrier function and the p-splines framework as the sufficient statistics basis, that combine the flexible B-splines basis with a ridge penalty parameter  $\lambda$  on differences of neighboring coefficients that controls the roughness of the resulting model. First proposed by [Eilers and Marx \(1996\)](#), p-splines are very flexible, smooth, and can be generalized to many settings. They consist of using a high number of equally spaced knots for the B-spline basis, which we then use in a poisson regression model. To control overfitting and give a smooth result, constraints on the discrete differences between coefficients of neighboring basis functions are imposed, which require tuning. In 1D, the problem consists of minimizing

$$- \text{Poisson loglikelihood}(s, B\theta) + \lambda \|D_q\theta\|^2, \quad (10)$$

where  $B$  is the matrix of transformed  $y_k$  to the B-spline basis,  $\theta$  are the parameters to estimate, and  $q$  is the degree of finite differences used for smoothing through the penalty term. For more details, [Eilers and Marx \(2021\)](#) and [Eilers et al. \(2015\)](#) give an overview of p-splines and many of its extensions, with the former also showcasing many applications that can be replicated in the book’s accompanying R package `JOPS` ([Eilers et al., 2021](#)).

## 7.1 Geographical distribution of *Bradypus variegatus*

To illustrate the use of the CB error estimator in this setting, we consider the problem of estimating the distribution of *Bradypus variegatus*, a lowland species of sloth, across Central and South America ([Phillips](#)

et al., 2006). Each data point consists of a latitude and longitude pair and represents a site where a sloth was seen, and the dataset consists of sighting of 116 sloths. We use a cubic 2D p-spline basis where the latitude and longitude axis have 30 knots each. To apply Lindsey’s method and get the Poisson counts, we divide the data in a 2d histogram of  $200 \times 200$  bins.

The 2D p-spline is detailed in Eilers et al. (2006) and Eilers and Marx (2003). It consists of a generalization of the problem in Equation 10, where  $B = B_1 \otimes B_2$  being the Kronecker product of matrices of marginal B-spline basis for each dimension (latitude and longitude). The penalty term is given by

$$P = \lambda_1 I_{c_1} \otimes D_1^T D_1 + \lambda_2 D_2^T D_2 \otimes I_{c_2},$$

where  $D_1$  and  $D_2$  are the discrete difference matrices for each dimension. If we assume  $\lambda_1 = \lambda_2$ , we have an isotropic penalty. Otherwise, we have an anisotropic penalty. The larger the values of  $\lambda_x$  and  $\lambda_z$ , the smoother the density will be. We tune  $\lambda_1$  and  $\lambda_2$  using CB.

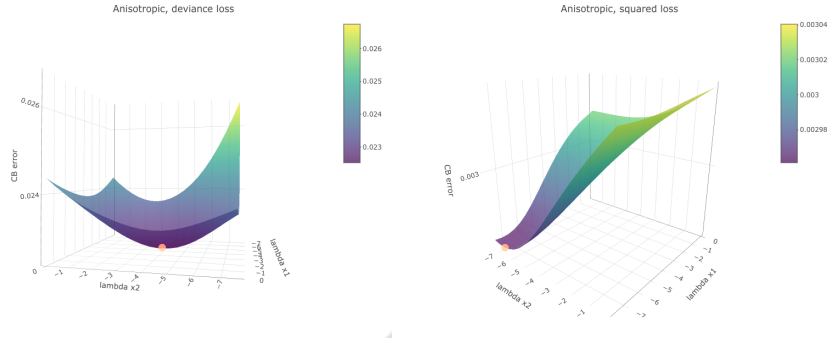
For the anisotropic penalty, we consider a different hyperparameter for latitude and longitude,  $\lambda_1$  and  $\lambda_2$  and  $20 \times 20$  different hyperparameter values, each varying from 0.001 to 1.5. In the isotropic setting, we set a common penalty parameter for both dimensions,  $\lambda = \lambda_1 = \lambda_2$ , and consider a sequence of 30 values for  $\lambda$  ranging from 0.001 to 5. For each hyperparameter value, we fit the Poisson regression model using the 2D p-spline regression and second order differences penalties, resulting in estimated probability values for all bins. Because we know that sloths only live in land, we set the probability of all bins that fully overlap with the ocean area to 0 and renormalize the estimated probabilities. Finally, we estimate out of sample error, perform model selection, and refit the selected model with the original data.

Error curves are in Figure 9. In both anisotropic and isotropic settings, squared loss minimization lead to much lower tuning parameter values, therefore using deviance loss lead to a more regularized density estimate. In this example, the minimizers of isotropic and anisotropic settings resulted in similar estimated deviance error, and the anisotropic penalty minimizer had similar values in both directions ( $\approx 0.2$ ), reducing the anisotropic penalty to an isotropic one. Figure 10 shows the datapoints (red) and the level curves of the fitted densities with optimal tuning parameter values (blue). The overfitting model selected by the squared error minimization results in the concentrated level curves of plots in the second row, while the deviance-error minimizer lead to a more smooth and intuitive density estimate.

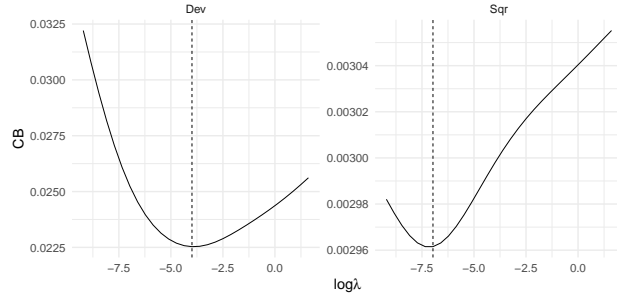
**Remark 7.** The fact that squared error lead to the selection of an overfitting model is not unexpected. Through many simulations, we found that squared loss is less robust to set-ups where there are many neighboring bins with drastically different counts, in particular many bins with 0. This commonly happens when the number of bins is large and the data is discrete, either by its nature or due to a discretization through data collection tools. In a univariate setting, this can be overcome by decreasing the number of bins. In the bivariate setting, however, decreasing the number of bins affects the bin width a lot, leading to a ‘pixelized’ result, affecting smoothness and visualization.

## 8 Discussion

We proposed the CB out-of-sample error estimator in the Poisson means problem as an alternative for the Unbiased Estimator, a direct consequence of Hudson’s Lemma. Our estimator is unbiased to a shrunken target  $\text{Err}_p$ , the out-of-sample error when the mean of the Poisson response is shrunken from  $\mu$  to  $\mu(1 - p)$ . We proved two limiting results when  $p \rightarrow 0$ : first, the new target parameter  $\text{Err}_p$  smoothly converges to  $\text{Err}$ , the original target of interest. Second, in an infinite bootstrap setting, the CB estimator fully recovers UE, under the same integrability assumptions on  $g$ . Through a bias-variance decomposition, we found that the MSE of our estimator can be fully controlled by  $B$ : with high enough finite  $B$ , the MSE of our estimator is well behaved. Our estimator performed well in simulated settings, in image denoising, and in density estimation. Our main advantage is that while UE requires the algorithm being evaluated to be refitted  $n + 1$  times, CB requires a fixed number of  $B$  refits, using less computational power when one considers problems with large datasets. Moreover, due to the optimal  $B$ ’s dependence on the magnitude of the mean, our estimator has particularly low computational cost for low SNR problems, a common setting in signal processing where variance stabilizing transformations are not applicable.



(a) Anisotropic penalty, deviance loss      (b) Anisotropic penalty, squared loss



(c) Isotropic penalty

Figure 9: Estimated error via CB for different tuning parameter values.

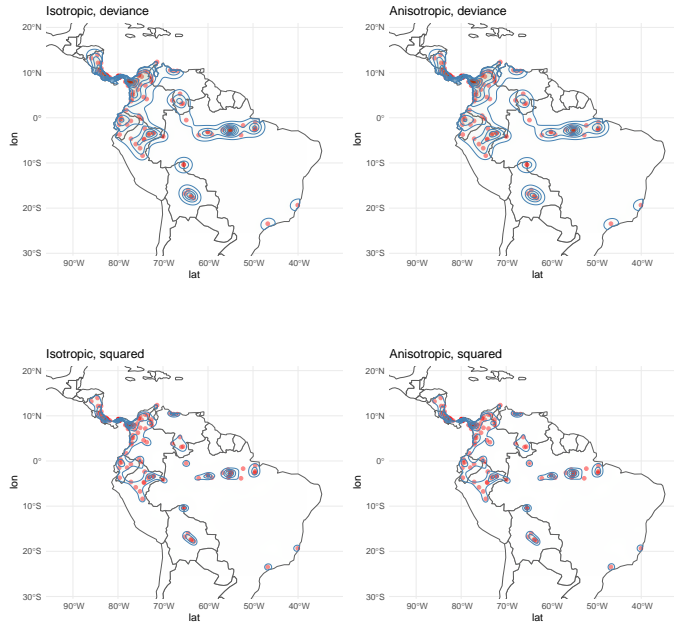


Figure 10: Contours for estimated probability function via Lindsey's method. Density on Figure (1,1) is optimal with respect to deviance CB error and isotropic penalty. Density on Figure (1,2) is optimal with respect to deviance CB error and anisotropic penalty. Density on Figure (2,1) is optimal with respect to squared CB error and isotropic penalty. Density on Figure (2,2) is optimal with respect to squared CB error and anisotropic penalty.

We finish by addressing three points. First, we consider variance stabilizing transformations and how to incorporate CB in that approach. Then, we discuss noise generation when performing hyperparameter tuning. At last, we briefly go over how one can extend the CB framework to other distributions.

**Variance stabilizing transformations** Because there are more algorithms that are tailored for the estimation of means in an additive Gaussian noise setting, a common procedure in the presence of Poisson response consists of transforming the data using a variance-stabilizing transformation, tune the methods by squared loss minimization, and transform the results back to the Poisson scale (Anscombe, 1948; Fryzlewicz and Nason, 2004; Brown et al., 2009; Fryzlewicz, 2018). This is known as the variance stabilizing transformation approach (VST), and is used in multiple applications. Brown et al. (2009)’s root-unroot method for density estimation is based on these ideas, combined with the discretization of the space proposed in Lindsey’s method, and Dupé et al. (2009); Makitalo and Foi (2009); Azzari and Foi (2016); Zhang et al. (2019) use VST in signal denoising problems. One common criticism to VST is its poor performance when the mean of the response is small, leading to a poor Gaussian approximation to the distribution of the transformed variable. Although it is not our focus to discuss and evaluate the quality and use cases of these approximations, we show how to use VST together with CB.

Let  $\eta : \mathbb{R}^n \rightarrow \mathbb{R}^n$  be an element-wise VST (usually a square root-like transformation) and  $g_\lambda$  an algorithm of interested tailored for Gaussian denoising with tuning parameter  $\lambda$ . Assume our response variable  $Y \in \mathbb{R}^n$  is Poisson distributed, we want to use  $g_\lambda$  to denoise  $Y$ , and need to tune  $\lambda$ . The standard approach is to transform  $Y$  using the VST, resulting in  $Z = \eta(Y)$ , select  $\hat{\lambda}$  that minimizes some out-of-sample error estimate of  $g_\lambda(Z)$ , and return predicted values  $\eta^{-1}(g_{\hat{\lambda}}(Z))$ . Training is being performed in the transformed data, which is desirable since the algorithm  $g$  is tailored to the Gaussian setting. However, the model selection step is also done targeting an optimal performance for random variable  $Z$ , and not  $Y$ , which is our variable of interest. The goal of VSTs is to allow the use of a known and good  $g$  for Gaussian response to a scenario where the response is Poisson, and produce good predictions of  $Y$ . With that in mind, we propose to incorporate the VST in the algorithm  $g$ , resulting in  $g_\lambda^*(Y) = (\eta^{-1} \circ g_\lambda \circ \eta)(Y)$ . Tuning is performed by minimizing CB (with either deviance or squared loss) directly on the original scale, ensuring that  $\hat{\lambda}$  is optimal for the original prediction task of interest.

**Random versus fixed noise when tuning parameters** In order to compute the CB estimator, we generate  $B$  samples of  $\omega|Y$ . In settings where the function  $g$  depends on a parameter  $\lambda$  and we are interested in tuning, we chose to use the same  $B$  samples of  $\omega|Y$  to compute CB for all considered values of  $\lambda$ . This choice leads to lower variability on CB across different values of  $\lambda$  and results on a smoother error curve of  $\lambda$  versus CB, however it implies on a dependency between CB estimates across different values  $\lambda$ . The question of whether this is a good or bad choice is not limited to the CB error estimation process, and can also be framed in terms of k-fold cross validation: should one divide the data into folds once and use the same fixed folds across different tuning parameter values, reducing variability but adding dependency, or should the folds be resampled for each tuning parameter? Comparing these two options and understanding their implications and theoretical properties is out of the scope of this paper, and we leave this investigation for future work.

**Extension to other distributions** The framework we presented targets estimating out-of-sample error in Poisson response problems. In this setting, CB’s construction heavily relies on Theorem 2, which for instance assumes that  $Y^*$  and  $Y^\dagger$  are defined per Lemma 2. While the full distribution of  $Y^*$  and  $Y^\dagger$  are important to derive most of the results in the paper, the unbiasedness property from Theorem 2, which is our starting point, only relies on two distributional properties of the coupled bootstrap samples:  $Y^* \perp Y^\dagger$  and  $\mathbb{E}[Y^*] = \mathbb{E}[Y^\dagger]$ . Therefore, in order to apply the CB framework to other distributions, it only requires searching for other generating schemes that satisfy these two properties.

## Acknowledgements

The authors thank Aaditya Ramdas and Boyan Duan for pointing out the decomposition from Lemma 2. NLO was supported by an Amazon Fellowship.

## References

- Hirotsugu Akaike. Information theory and an extension of the maximum likelihood principle. In *Second International Symposium on Information Theory*, pages 267–281, 1973.
- F. J. Anscombe. The transformation of poisson, binomial and negative-binomial data. *Biometrika*, 35(3-4): 246–254, 12 1948. ISSN 0006-3444. doi: 10.1093/biomet/35.3-4.246. URL <https://doi.org/10.1093/biomet/35.3-4.246>.
- Lucio Azzari and Alessandro Foi. Variance stabilization for noisy+estimate combination in iterative poisson denoising. *IEEE Signal Processing Letters*, 23(8):1086–1090, 2016. doi: 10.1109/LSP.2016.2580600.
- James Berger. Improving on inadmissible estimators in continuous exponential families with applications to simultaneous estimation of gamma scale parameters. *The Annals of Statistics*, 8(3):545–571, 1980. ISSN 00905364. URL <http://www.jstor.org/stable/2240592>.
- Leo Breiman. The little bootstrap and other methods for dimensionality selection in regression: X-fixed prediction error. *Journal of the American Statistical Association*, 87(419):738–754, 1992.
- Lawrence Brown, Tony Cai, Ren Zhang, Linda Zhao, and Harrison Zhou. The root–unroot algorithm for density estimation as implemented via wavelet block thresholding. *Probability Theory and Related Fields*, 146(3):401, 2009. doi: 10.1007/s00440-008-0194-2. URL <https://doi.org/10.1007/s00440-008-0194-2>.
- Lawrence D. Brown, Eitan Greenshtein, and Ya’acov Ritov. The poisson compound decision problem revisited. *Journal of the American Statistical Association*, 108(502):741–749, 2013. doi: 10.1080/01621459.2013.771582. URL <https://doi.org/10.1080/01621459.2013.771582>.
- Yang Cao and Yao Xie. Poisson matrix recovery and completion. *IEEE Transactions on Signal Processing*, 64(6):1609–1620, 2016. doi: 10.1109/TSP.2015.2500192.
- Charles-Alban Deledalle. Estimation of Kullback-Leibler losses for noisy recovery problems within the exponential family. *Electronic Journal of Statistics*, 11(2):3141–3164, 2017.
- François-Xavier Dupé, J.M. Fadili, and Jean-Luc Starck. A proximal iteration for deconvolving poisson noisy images using sparse representations. *Image Processing, IEEE Transactions on*, 18:310 – 321, 03 2009. doi: 10.1109/TIP.2008.2008223.
- Bradley Efron. The estimation of prediction error: Covariance penalties and cross-validation. *Journal of the American Statistical Association*, 99(467):619–632, 2004.
- Bradley Efron and Robert Tibshirani. Using specially designed exponential families for density estimation. *The Annals of Statistics*, 24(6):2431–2461, 1996. ISSN 00905364. URL <http://www.jstor.org/stable/2242691>.
- Paul Eilers and Brian Marx. Multivariate calibration with temperature interaction using two-dimensional penalized signal regression. *Chemometrics and Intelligent Laboratory Systems*, 66:159–174, 06 2003. doi: 10.1016/S0169-7439(03)00029-7.
- Paul Eilers, Brian Marx, and María Durbán. Twenty years of p-splines. *SORT (Statistics and Operations Research Transactions)*, 39:149–186, 01 2015.
- Paul Eilers, Brian Marx, Bin Li, Jutta Gampe, and Maria Xose Rodriguez-Alvarez. *JOPS: Practical Smoothing with P-Splines*, 2021. URL <https://CRAN.R-project.org/package=JOPS>. R package version 0.1.15.
- Paul H. C. Eilers and Brian D. Marx. Flexible smoothing with B-splines and penalties. *Statistical Science*, 11(2):89 – 121, 1996. doi: 10.1214/ss/1038425655. URL <https://doi.org/10.1214/ss/1038425655>.
- Paul H.C. Eilers and Brian D. Marx. *Practical Smoothing: The Joys of P-splines*. Cambridge University Press, 2021. doi: 10.1017/9781108610247.

- Paul H.C. Eilers, Iain D. Currie, and Maria Durban. Fast and compact smoothing on large multidimensional grids. *Computational Statistics & Data Analysis*, 50(1):61–76, 2006. ISSN 0167-9473. doi: <https://doi.org/10.1016/j.csda.2004.07.008>. URL <https://www.sciencedirect.com/science/article/pii/S0167947304002270>. 2nd Special issue on Matrix Computations and Statistics.
- Piotr Fryzlewicz. Likelihood ratio haar variance stabilization and normalization for poisson and other non-gaussian noise removal. *Statistica Sinica*, 28(4):2885–2901, 2018. ISSN 10170405, 19968507. URL <https://www.jstor.org/stable/26511242>.
- Piotr Fryzlewicz and Guy P Nason. A haar-fisz algorithm for poisson intensity estimation. *Journal of Computational and Graphical Statistics*, 13(3):621–638, 2004. doi: 10.1198/106186004X2697. URL <https://doi.org/10.1198/106186004X2697>.
- Zijun Gao and Trevor Hastie. Lincede: Conditional density estimation via lindsey’s method, 2021. URL <https://arxiv.org/abs/2107.12713>.
- Malay Ghosh, Jiunn Tzon Hwang, and Kam-Wah Tsui. Construction of improved estimators in multiparameter estimation for discrete exponential families. *The Annals of Statistics*, 11(2):351–367, 1983. ISSN 00905364. URL <http://www.jstor.org/stable/2240551>.
- Zachary T. Harmany, Roummel F. Marcia, and Rebecca M. Willett. Sparse poisson intensity reconstruction algorithms. In *2009 IEEE/SP 15th Workshop on Statistical Signal Processing*, pages 634–637, 2009. doi: 10.1109/SSP.2009.5278495.
- Zachary T. Harmany, Roummel F. Marcia, and Rebecca M. Willett. This is spiral-tap: Sparse poisson intensity reconstruction algorithms—theory and practice. *IEEE Transactions on Image Processing*, 21(3):1084–1096, 2012. doi: 10.1109/TIP.2011.2168410.
- H. Malcolm Hudson. A natural identity for exponential families with applications in multiparameter estimation. *Annals of Statistics*, 6(3):473–484, 05 1978.
- Jiunn Tzon Hwang. Improving Upon Standard Estimators in Discrete Exponential Families with Applications to Poisson and Negative Binomial Cases. *The Annals of Statistics*, 10(3):857 – 867, 1982. doi: 10.1214/aos/1176345876. URL <https://doi.org/10.1214/aos/1176345876>.
- Yoann Le Montagner, Elsa D. Angelini, and Jean-Christophe Olivo-Marin. An unbiased risk estimator for image denoising in the presence of mixed poisson–gaussian noise. *IEEE Transactions on Image Processing*, 23(3):1255–1268, 2014. doi: 10.1109/TIP.2014.2300821.
- James Leiner, Boyan Duan, Larry Wasserman, and Aaditya Ramdas. Data fission: splitting a single data point, 2021. URL <https://arxiv.org/abs/2112.11079>.
- J. K. Lindsey. Comparison of probability distributions. *Journal of the Royal Statistical Society. Series B (Methodological)*, 36(1):38–47, 1974. ISSN 00359246. URL <http://www.jstor.org/stable/2984768>.
- J.K. Lindsey and G. Mersch. Fitting and comparing probability distributions with log linear models. *Computational Statistics & Data Analysis*, 13(4):373–384, 1992. ISSN 0167-9473. doi: [https://doi.org/10.1016/0167-9473\(92\)90112-S](https://doi.org/10.1016/0167-9473(92)90112-S). URL <https://www.sciencedirect.com/science/article/pii/016794739290112S>.
- Daniel J Lingenfelter, Jeffrey A. Fessler, and Zhong He. Sparsity regularization for image reconstruction with Poisson data. In Charles A. Bouman, Eric L. Miller, and Ilya Pollak, editors, *Computational Imaging VII*, volume 7246, pages 96 – 105. International Society for Optics and Photonics, SPIE, 2009. doi: 10.1117/12.816961. URL <https://doi.org/10.1117/12.816961>.
- Florian Luisier, Cédric Vonesch, Thierry Blu, and Michael Unser. Fast interscale wavelet denoising of poisson-corrupted images. *Signal Processing*, 90(2):415–427, 2010. ISSN 0165-1684. doi: <https://doi.org/10.1016/j.sigpro.2009.07.009>. URL <https://www.sciencedirect.com/science/article/pii/S0165168409003016>.

- Markku Makitalo and Alessandro Foi. On the inversion of the anscombe transformation in low-count poisson image denoising. In *2009 International Workshop on Local and Non-Local Approximation in Image Processing*, pages 26–32, 2009. doi: 10.1109/LNLA.2009.5278406.
- Natalia L. Oliveira, Jing Lei, and Ryan J. Tibshirani. Unbiased risk estimation in the normal means problem via coupled bootstrap techniques. 2021. doi: 10.48550/ARXIV.2111.09447. URL <https://arxiv.org/abs/2111.09447>.
- Steven J. Phillips, Robert P. Anderson, and Robert E. Schapire. Maximum entropy modeling of species geographic distributions. *Ecological Modelling*, 190(3):231–259, 2006. ISSN 0304-3800. doi: <https://doi.org/10.1016/j.ecolmodel.2005.03.026>. URL <https://www.sciencedirect.com/science/article/pii/S030438000500267X>.
- Maxim Raginsky, Rebecca M. Willett, Zachary T. Harmany, and Roummel F. Marcia. Compressed sensing performance bounds under poisson noise. *IEEE Transactions on Signal Processing*, 58(8):3990–4002, 2010. doi: 10.1109/TSP.2010.2049997.
- Joseph Salmon, Zachary Harmany, Charles-Alban Deledalle, and Rebecca Willett. Poisson noise reduction with non-local pca. *Journal of Mathematical Imaging and Vision*, 48(2):279–294, 2014. doi: 10.1007/s10851-013-0435-6. URL <https://doi.org/10.1007/s10851-013-0435-6>.
- Xiaotong Shen, Hsin-Cheng Huang, and Jimmy Ye. Adaptive model selection and assessment for exponential family distributions. *Technometrics*, 46(3):306–317, 2004. doi: 10.1198/004017004000000338. URL <https://doi.org/10.1198/004017004000000338>.
- Charles Stein. Estimation of the mean of a multivariate normal distribution. *Annals of Statistics*, 9(6): 1135–1151, 1981.
- Ryan J. Tibshirani. Degrees of freedom and model search. *Statistica Sinica*, 25(3):1265–1296, 2015.
- Ryan J. Tibshirani and Saharon Rosset. Excess optimism: How biased in the apparent error rate of a SURE-tuned prediction rule? *Journal of the American Statistical Association*, 114(526):697–712, 2019.
- Jianming Ye. On measuring and correcting the effects of data mining and model selection. *Journal of the American Statistical Association*, 93(441):120–131, 1998.
- Minghui Zhang, Fengqin Zhang, Qiegen Liu, and Shanshan Wang. Vst-net: Variance-stabilizing transformation inspired network for poisson denoising. *Journal of Visual Communication and Image Representation*, 62:12–22, 2019. ISSN 1047-3203. doi: <https://doi.org/10.1016/j.jvcir.2019.04.011>. URL <https://www.sciencedirect.com/science/article/pii/S1047320319301439>.

## A Differences between deviance and squared loss for the empirical Bayes estimator

An interesting example that shows similarities and differences between the two losses is the empirical Bayes (EB) estimator for the mean of the Poisson compound problem. [Brown et al. \(2013\)](#) focuses on improving the EB estimator of the many Poisson means problem under squared loss. Let  $Y_i \sim \text{Poisson}(\mu_i), i \in [n]$ . Assuming  $\mu_1, \dots, \mu_n$  are iid samples from  $\Lambda \sim G$ , the EB estimator is  $\hat{\mu}(Y) = \operatorname{argmin}_{\mu} \mathbb{E}[l(\Lambda, \hat{\mu}(Y))]$ . For both squared and deviance loss, the minimizer is the same, resulting in the same EB estimator

$$\hat{\mu}(y) = \mathbb{E}[\Lambda | Y = y] = (y + 1) \frac{\#\{i : Y_i = y + 1\}}{\#\{i : Y_i = y\}}.$$

[Brown et al. \(2013\)](#) proposes a 3-step improvement to this estimator, and for our example we will only consider the first step, which consists of smoothing the EB estimator via a corruption parameter  $h$ . Assume

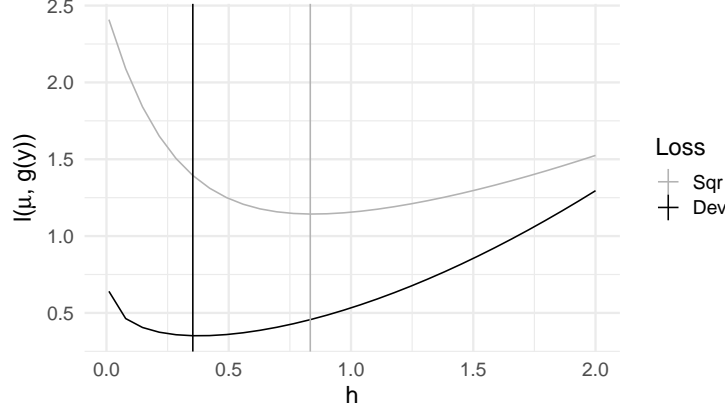


Figure 11:  $h$  versus risk for the two different loss function, Larry Brown's step 1 EB estimator.

$N \sim \text{Poisson}(h)$ ,  $N \perp Y, \Lambda$ . Let  $Z = N + Y$ . Define  $\mu_{h,1} = \mathbb{E}[\Lambda|Z = z] = \mathbb{E}[\Lambda + h|Z = z] - h$ . For a given smoothing parameter  $h$ ,  $\mu_{h,1}$  is optimal for the corrupted observations. This leads to the estimator

$$\hat{\mu}_{h,1}(z) = (z + 1) \frac{\tilde{P}_Z(z + 1)}{\tilde{P}_Z(z)} - h,$$

where  $P_Z(z) = \sum_{i=0}^z \hat{P}_Y(i) \times e^{-h} h^{z-i} / (z - i)!$ . To see the difference in optimal  $h$  for each loss, consider the following experimental set-up: sample size is 1000,  $\mu_1 = \dots = \mu_{100} = 7.5$  and  $\mu_{101} = \dots = \mu_{1000} = 1$ . Figure 11 shows the curves of  $h$  versus  $\sum_{i=1}^{1000} \text{Sqr}(\mu, \hat{\mu}_{h,1}(z_i)) / 1000$  and  $\sum_{i=1}^{1000} \text{Dev}(\mu, \hat{\mu}_{h,1}(z_i)) / 1000$ , and the vertical lines are at the optimal  $h$  for each loss. In sum, although the two loss functions lead to the same EB estimator and the step-1 improvement was the same in both cases, hyperparameter tuning using the two loss functions can lead to very different models.

## B Proof of Theorem 1

*Proof.* Starting from Efron (2004) Optimism Theorem,

$$\begin{aligned} \mathbb{E}[D_\phi(\tilde{Y}_i, g_i(Y))] &= \mathbb{E}[D_\phi(Y_i, g_i(Y))] + \text{Cov}[-\phi'(g_i(Y)), Y_i] && \text{(Opt. Thm.)} \\ &= \mathbb{E}[\phi(Y_i) - \phi(g_i(Y)) - \phi'(g_i(Y))(Y_i - g_i(Y))] - \mathbb{E}[\phi'(g_i(Y))Y_i] \\ &\quad + \mathbb{E}[\phi'(g_i(Y))]\mu_i \\ &= \mathbb{E}[\phi(Y_i) - \phi(g_i(Y)) - \phi'(g_i(Y))(Y_i - g_i(Y))] - \phi'(g_i(Y))Y_i \\ &\quad + \mathbb{E}[Y_i \phi'(g_i(Y - e_i))] && \text{(Lemma 1)} \\ &= \mathbb{E}[\phi(Y_i) - \phi(g_i(Y)) - 2\phi'(g_i(Y))Y_i + \phi'(g_i(Y))g_i(Y) \\ &\quad + Y_i \phi'(g_i(Y - e_i))]. \end{aligned}$$

□

## C Diverging deviance for the CB and UE estimators

The unbiased estimator (through Hudson's Lemma) and deviance error itself require  $\mathbb{E}[\log g(Y)] < \infty$ , and CB requires  $\mathbb{E}[Y^\dagger \log g(Y^*)] < \infty$ , which are both automatically violated if  $g$  maps any value of  $y$  to 0. While  $g(y) \in [0, \infty)$  is problematic for both unbiased and CB estimators, they rely on different assumptions. Assuming that  $g$  passes through the origin and that  $p$  is small, the probability of observing a value of  $y$  that results in a diverging unbiased estimator is higher than observing a value of  $y$  that results in a diverging CB estimator. Recall that the problematic term in the unbiased estimator is  $Y \log g(Y - 1)$  and for functions

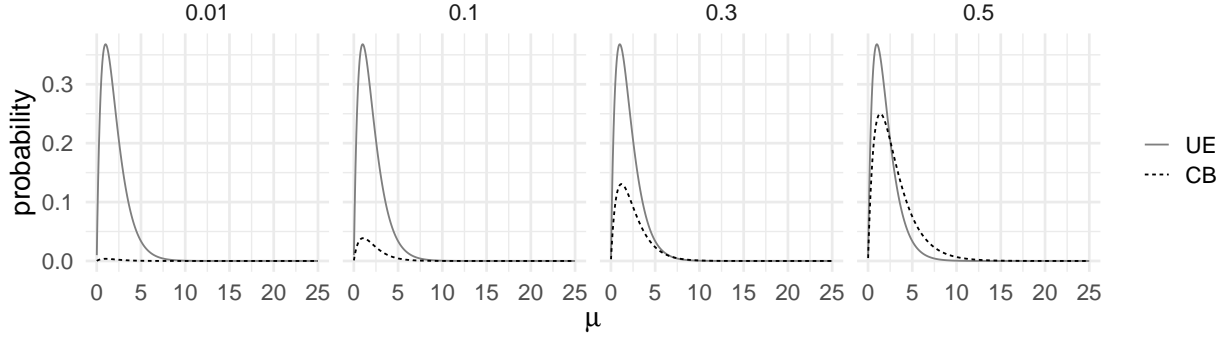


Figure 12: True mean  $\mu$  versus the probability of observing a diverging term for the unbiased estimator (continuous gray line) and CB (dotted black line). From left to right, the considered values of  $p$  are 0.01, 0.1, 0.3, and 0.5.

$g$  that pass through the origin. When  $Y = 0$ , the term is 0, and when  $Y = 1$  we have the problem term  $1 \log 0$ . Therefore, a diverging unbiased estimate happens whenever we observe  $Y = 1$ . Now, with CB, the problem lies in a similar term:  $Y^\dagger \log g(Y^*)$ , and we run into an issue whenever  $Y^* = 0$  and  $Y^\dagger \neq 0$ . Note that when  $Y = 0$ , both  $Y^\dagger = Y^* = 0$ , so we do not have that problem. What is the probability that these events happen?

$$\begin{aligned}
\mathbb{P}(\text{diverging UE}) &= \mathbb{P}(Y = 1) = e^{-\mu} \mu. \\
\mathbb{P}(\text{diverging CB}) &= \sum_{y=1}^{\infty} \mathbb{P}(Y^* = 0 | Y = y) \mathbb{P}(Y = y) \\
&= \sum_{y=1}^{\infty} \mathbb{P}(\omega = Y | Y = y) \mathbb{P}(Y = y) \\
&= \sum_{y=1}^{\infty} p^y e^{-\mu} \mu^y / y! = \sum_{y=1}^{\infty} e^{-\mu + p\mu - p\mu} (p\mu)^y / y! \\
&= e^{-\mu + p\mu} (1 - \mathbb{P}(U = 0)) \quad (U \sim \text{Poisson}(p\mu)) \\
&= e^{-\mu} (e^{p\mu} - 1).
\end{aligned}$$

To compare the two probabilities, we plot them for different values of the true mean  $\mu$  and considering 4 values of  $p$ : 0.01, 0.1, 0.3, and 0.5. Figure 12 shows the curves. For small  $p$ , our estimator has much lower probability of sampling a problematic point than the unbiased estimator.

## D Proof of Lemma 2

*Proof.* Let  $(U, V) = (g_1(Y, \omega), g_2(Y, \omega)) = (Y - \omega, \omega)$ . The joint pmf of  $(Y, \omega)$  is given by

$$\begin{aligned}
\mathbb{P}(Y = y, \omega = \omega) &= \mathbb{P}(\omega = \omega | Y = y) \mathbb{P}(Y = y) \\
&= \binom{y}{\omega} p^\omega (1-p)^{y-\omega} \frac{\mu^y e^{-\mu}}{y!}, \text{ for } \omega = 0, \dots, y, y \geq 0.
\end{aligned}$$

Now we want to find the joint distribution of the random vector  $(U, V)$ , a bivariate transformation of  $(Y, \omega)$ .

$$\mathbb{P}(U = u, V = v) = \sum_{(y, \omega) \in A_{u, v}} \mathbb{P}(Y = y, \omega = \omega),$$

where  $A_{u,v} = \{(y, \omega) : u = y - \omega, v = \omega\} = \{(u + v, v)\}$ , since the transformation is a one-to-one mapping. Then,

$$\begin{aligned} \mathbb{P}(U = u, V = v) &= \mathbb{P}(Y = u + v, \omega = v) \\ &= \binom{u+v}{v} p^v (1-p)^u \frac{\mu^{u+v} e^{-\mu}}{(u+v)!} \\ &= \frac{1}{u!v!} p^v (1-p)^u \mu^u \mu^v e^{-\mu(p+1-p)} \\ &= \frac{(\mu(1-p))^u e^{-\mu p}}{u!} \frac{(\mu p)^v e^{-\mu(1-p)}}{v!}. \end{aligned}$$

□

## E Proof of Theorem 2

*Proof.* Equation (4) follows from a direct application of Lemma 3. For the quadratic loss result, plug in  $b(x) = \|x\|_2^2$  in (4). For the deviance loss result, let  $\phi(x) = \langle 2x, (\log x - 1) \rangle$ . Then, from (4),

$$\begin{aligned} \text{Err}_p^{(\text{Dev})}(g) &= \mathbb{E}[\text{Dev}(\tilde{Y}^*, g(Y^*))] = 2 \sum_{i=1}^n \mathbb{E}[(Y_i^\dagger \log \frac{Y_i^\dagger}{g_i(Y^*)} - Y_i^\dagger + g_i(Y^*)) \\ &\quad - Y_i^\dagger (\log Y_i^\dagger - 1) + Y_i^* (\log Y_i^* - 1)] \\ &= 2 \sum_{i=1}^n \mathbb{E}[Y_i^\dagger \log Y_i^\dagger - Y_i^\dagger \log g_i(Y^*) - Y_i^\dagger + g_i(Y^*) \\ &\quad - Y_i^\dagger \log Y_i^\dagger + Y_i^\dagger + Y_i^* \log Y_i^* - Y_i^*] \\ &= 2 \sum_{i=1}^n \mathbb{E}[Y_i^* \log Y_i^* - Y_i^\dagger \log g_i(Y^*) + g_i(Y^*) - Y_i^*] \\ &= \mathbb{E}[\text{CB}_p^{(\text{Dev})}] \end{aligned}$$

with  $B = 1$ . The result follows directly for larger  $B$ . □

## F Proof of Proposition 1

*Proof.* First, we show that the map is continuous. For any  $p \in [0, 1)$ ,

$$\begin{aligned} \lim_{t \rightarrow p} \mathbb{E}[f(\tilde{Y}_p, Y_p)] &= \lim_{t \rightarrow p} \sum_{y_1, \dots, y_n=0}^{\infty} \sum_{\tilde{y}_1, \dots, \tilde{y}_n=0}^{\infty} f(y, \tilde{y}) \frac{e^{-2(1-t) \sum_{i=1}^n \mu_i} (\prod_{i=1}^n \mu_i^{\tilde{y}_i + y_i}) (1-t)^{\sum_{i=1}^n \tilde{y}_i + y_i}}{\prod_{i=1}^n \tilde{y}_i! y_i!} \\ &= \sum_{y_1, \dots, y_n=0}^{\infty} \sum_{\tilde{y}_1, \dots, \tilde{y}_n=0}^{\infty} f(y, \tilde{y}) \frac{e^{-2(1-p) \sum_{i=1}^n \mu_i} (\prod_{i=1}^n \mu_i^{\tilde{y}_i + y_i}) (1-p)^{\sum_{i=1}^n \tilde{y}_i + y_i}}{\prod_{i=1}^n \tilde{y}_i! y_i!} \end{aligned}$$

To switch the infinite sum and the limit, we used DCT. The dominating function is given by

$$h(\tilde{y}, y) = f(y, \tilde{y}) \frac{\prod_{i=1}^n \mu_i^{\tilde{y}_i + y_i}}{\prod_{i=1}^n \tilde{y}_i! y_i!}$$

which is integrable by assumption:

$$\begin{aligned} \sum_{y_1, \dots, y_n=0}^{\infty} \sum_{\tilde{y}_1, \dots, \tilde{y}_n=0}^{\infty} h(\tilde{y}, y) &= \sum_{y_1, \dots, y_n=0}^{\infty} \sum_{\tilde{y}_1, \dots, \tilde{y}_n=0}^{\infty} f(y, \tilde{y}) \frac{\prod_{i=1}^n \mu_i^{\tilde{y}_i + y_i}}{\prod_{i=1}^n \tilde{y}_i! y_i!} e^{-2 \sum_{i=1}^n \mu_i} e^{2 \sum_{i=1}^n \mu_i} \\ &= e^{2 \sum_{i=1}^n \mu_i} \mathbb{E}[f(Y_0, \tilde{Y}_0)] < \infty. \end{aligned}$$

For the first derivative, note that

$$\begin{aligned}
\frac{\partial \mathbb{E}[f(Y_p, \tilde{Y}_p)]}{\partial p} &= \frac{\partial}{\partial p} \sum_{y_1, \dots, y_n=0}^{\infty} \sum_{\tilde{y}_1, \dots, \tilde{y}_n=0}^{\infty} f(y, \tilde{y}) \frac{e^{-2(1-p) \sum_{i=1}^n \mu_i} \prod_{i=1}^n \mu_i^{\tilde{y}_i + y_i} (1-p)^{\sum_{i=1}^n \tilde{y}_i + y_i}}{\prod_{i=1}^n \tilde{y}_i! y_i!} \\
&= \sum_{y_1, \dots, y_n=0}^{\infty} \sum_{\tilde{y}_1, \dots, \tilde{y}_n=0}^{\infty} \frac{f(y, \tilde{y}) \prod_{i=1}^n \mu_i^{\tilde{y}_i + y_i}}{\prod_{i=1}^n \tilde{y}_i! y_i!} \frac{\partial}{\partial p} e^{-2(1-p) \sum_{i=1}^n \mu_i} (1-p)^{\sum_{i=1}^n \tilde{y}_i + y_i} \\
&= \sum_{y_1, \dots, y_n=0}^{\infty} \sum_{\tilde{y}_1, \dots, \tilde{y}_n=0}^{\infty} \frac{f(y, \tilde{y}) \prod_{i=1}^n \mu_i^{\tilde{y}_i + y_i}}{\prod_{i=1}^n \tilde{y}_i! y_i!} \left( 2 \sum_{i=1}^n \mu_i e^{-2(1-p) \sum_{i=1}^n \mu_i} (1-p)^{\sum_{i=1}^n \tilde{y}_i + y_i} \right. \\
&\quad \left. - \sum_{i=1}^n (\tilde{y}_i + y_i) e^{-2(1-p) \sum_{i=1}^n \mu_i} (1-p)^{\sum_{i=1}^n \tilde{y}_i + y_i - 1} \right) \\
&= 2 \sum_{i=1}^n \mu_i \mathbb{E}[f(Y_p, \tilde{Y}_p)] - \frac{1}{(1-p)} \mathbb{E}[f(Y_p, \tilde{Y}_p) \langle \tilde{Y}_p + Y_p, 1 \rangle],
\end{aligned}$$

where we used Leibniz rule to switch the sums and derivative. To prove continuity of the first derivative, we apply the continuity result on  $\mathbb{E}[f(Y_p, \tilde{Y}_p) \langle \tilde{Y}_p + Y_p, 1 \rangle]$ . For up to the  $k^{\text{th}}$  derivatives, the argument follows from sequential applications of the continuity result and the derivative computation, with updated arguments.  $\square$

## G Proof of Theorem 3

We start by presenting Lemma 4, an important result that is used in the proof of Theorem 3.

**Lemma 4.** *Let  $h_i : \mathbb{N}_0^n \rightarrow \mathbb{R}^+$ , and define  $h_i(z) = 0$  for any  $z \notin \mathbb{N}_0^n$ . Let  $\omega$  and  $Y$  be as defined in Lemma 2 and assume that  $\mathbb{E}[|h_i(Y)|] < \infty$ . Then,*

- (a)  $\lim_{p \rightarrow 0} \mathbb{E}[h_i(Y - \omega) | Y] = h_i(Y)$
- (b)  $\lim_{p \rightarrow 0} \frac{1-p}{p} \mathbb{E}[\omega_i h_i(Y - \omega) | Y] = Y_i h_i(Y - e_i),$

where  $e_i$  is a vector in  $\mathbb{R}^n$  whose  $i^{\text{th}}$  entry is 1 and the other entries are 0.

*Proof.* Define the following sets:

$$\begin{aligned}
\Omega &= \{(\omega_1, \dots, \omega_n) : \omega_j \in \{0, \dots, Y_j\}, j \in [n]\}; \\
\Omega_{\setminus 0} &= \Omega \setminus \{(\omega_1, \dots, \omega_n) : \omega_j = 0, j \in [n]\}; \\
\Omega_{i0} &= \{(\omega_1, \dots, \omega_n) : \omega_i = 0, \omega_j \in \{0, \dots, Y_j\}, j \in [n] \setminus \{i\}\}; \\
\Omega_{i10} &= \{(\omega_1, \dots, \omega_n) : \omega_i = 1, \omega_j = 0, j \in [n] \setminus \{i\}\}; \\
\Omega_{i1\bar{0}} &= \{(\omega_1, \dots, \omega_n) : \omega_i \geq 1, \omega_j \in \{0, \dots, Y_j\}, j \in [n] \setminus \{i\}\} \setminus \Omega_{i10}.
\end{aligned}$$

For result (a), we have

$$\begin{aligned}
\lim_{p \rightarrow 0} \mathbb{E}[h_i(Y - \omega) | Y] &= \lim_{p \rightarrow 0} \sum_{\omega \in \Omega} h_i(Y - \omega) p^{\sum_{k=1}^n \omega_k} (1-p)^{\sum_{k=1}^n Y_k - \omega_k} \prod_{j=1}^n \binom{Y_j}{\omega_j} \\
&= \lim_{p \rightarrow 0} h_i(Y) (1-p)^{\sum_{k=1}^n Y_k} \\
&\quad + \sum_{\omega \in \Omega_{\setminus 0}} \lim_{p \rightarrow 0} h_i(Y - \omega) p^{\sum_{k=1}^n \omega_k} (1-p)^{\sum_{k=1}^n Y_k - \omega_k} \prod_{j=1}^n \binom{Y_j}{\omega_j} \\
&= \sum_{i=1}^n h_i(Y),
\end{aligned}$$

since for  $\omega \in \Omega_{\setminus 0}$ , we have that  $\sum_{k=1}^n \omega_k > 0$ .

For result (b),

$$\begin{aligned}
\lim_{p \rightarrow 0} \frac{1-p}{p} \mathbb{E}[\omega_i h_i(Y - \omega) | Y] &= \lim_{p \rightarrow 0} \frac{1-p}{p} \sum_{\omega \in \Omega} \omega_i h_i(Y - \omega) p^{\sum_{k=1}^n \omega_k} (1-p)^{\sum_{k=1}^n Y_k - \omega_k} \prod_{j=1}^n \binom{Y_j}{\omega_j} \\
&= \lim_{p \rightarrow 0} \sum_{\omega \in \Omega} \omega_i h_i(Y - \omega) p^{\sum_{k=1}^n \omega_k - 1} (1-p)^{1 + \sum_{k=1}^n Y_k - \omega_k} \prod_{j=1}^n \binom{Y_j}{\omega_j} \\
&= \lim_{p \rightarrow 0} \sum_{\omega \in \Omega_{i10}} \omega_i h_i(Y - \omega) p^{\sum_{k=1}^n \omega_k - 1} (1-p)^{1 + \sum_{k=1}^n Y_k - \omega_k} \prod_{j=1}^n \binom{Y_j}{\omega_j} \\
&= \lim_{p \rightarrow 0} h_i(Y - e_i) p^0 (1-p)^{1 + \sum_{k=1}^n Y_k - \omega_k} \binom{Y_i}{1} \prod_{j \neq i, j=1}^n \binom{Y_j}{0} \\
&= Y_i h_i(Y - e_i),
\end{aligned}$$

where we use the fact that  $\Omega = \Omega_{i0} \cup \Omega_{i10} \cup \Omega_{i1\bar{0}}$  and

$$\begin{aligned}
&\lim_{p \rightarrow 0} \sum_{\omega \in \Omega_{i0}} \omega_i h_i(Y - \omega) p^{\sum_{k=1}^n \omega_k - 1} (1-p)^{1 + \sum_{k=1}^n Y_k - \omega_k} \prod_{j=1}^n \binom{Y_j}{\omega_j} \\
&= \lim_{p \rightarrow 0} \sum_{\omega \in \Omega_{i0}} 0 h_i(Y - \omega) p^{\sum_{k=1}^n \omega_k - 1} (1-p)^{1 + \sum_{k=1}^n Y_k - \omega_k} \prod_{j=1}^n \binom{Y_j}{\omega_j} = 0 \\
&\lim_{p \rightarrow 0} \sum_{\omega \in \Omega_{i1\bar{0}}} \omega_i h_i(Y - \omega) p^{\sum_{k=1}^n \omega_k - 1} (1-p)^{1 + \sum_{k=1}^n Y_k - \omega_k} \prod_{j=1}^n \binom{Y_j}{\omega_j} \\
&= \sum_{\omega \in \Omega_{i1\bar{0}}} \omega_i h_i(Y - \omega) 0^{\sum_{k=1}^n \omega_k - 1} \prod_{j=1}^n \binom{Y_j}{\omega_j} = 0,
\end{aligned}$$

since for  $\omega \in \Omega_{i1\bar{0}}$ , we have that  $\sum_{k=1}^n \omega_k - 1 > 0$ . □

Now we present the proof of Theorem 3.

*Proof.* We start by expanding the infinite bootstrap estimator

$$\begin{aligned}
\mathbb{E}[\text{CB}_p(g) | Y] &= \sum_{i=1}^n \mathbb{E}[D_\phi(Y_i^\dagger, g_i(Y^*)) + \phi(Y_i^*) - \phi(Y_i^\dagger) | Y] \\
&= \sum_{i=1}^n \mathbb{E}[\phi(Y_i^*) - \phi(g_i(Y^*)) - \phi'(g_i(Y^*))(Y_i^\dagger - Y_i^*) | Y] \\
&= \sum_{i=1}^n \mathbb{E}[\phi(Y_i - \omega_i) - \phi(g_i(Y - \omega)) - \phi'(g_i(Y - \omega)) \left( \frac{1-p}{p} \omega_i - (Y_i - \omega_i) \right) | Y] \\
&= \sum_{i=1}^n \mathbb{E}[\phi(Y_i - \omega_i) - \phi(g_i(Y - \omega)) - \frac{(1-p)}{p} \phi'(g_i(Y - \omega)) \omega_i \\
&\quad + \phi'(g_i(Y - \omega))(Y_i - \omega_i) | Y].
\end{aligned}$$

Then, taking the limit,

$$\begin{aligned}
\lim_{p \rightarrow 0} \mathbb{E}[\text{CB}_p(g)|Y] &= \sum_{i=1}^n \lim_{p \rightarrow 0} \mathbb{E}[\phi(Y_i - \omega_i) - \phi(g_i(Y - \omega)) - \frac{(1-p)}{p} \phi'(g_i(Y - \omega))\omega_i \\
&\quad + \phi'(g_i(Y - \omega))(Y_i - \omega_i)|Y] \\
&= \sum_{i=1}^n \lim_{p \rightarrow 0} \mathbb{E}[\phi(Y_i - \omega_i) - \phi(g_i(Y - \omega)) \\
&\quad + \phi'(g_i(Y - \omega))(Y_i - \omega_i)|Y] - Y_i \phi'(g_i(Y - e_i)) \quad (\text{Lemma 4 (b)}) \\
&= \sum_{i=1}^n \phi(Y_i) - \phi(g_i(Y)) + \phi'(g_i(Y))(Y_i) - Y_i \phi'(g_i(Y - e_i)) \quad (\text{Lemma 4 (a)}) \\
&= \text{UE}(Y).
\end{aligned}$$

□

## H Proofs of propositions from Section 4

### H.1 Proof of Proposition 2

*Proof.* From Proposition 1, the mapping  $p \mapsto \text{Err}_p$  has continuous first derivatives for  $p \in [0, 1)$ . With an application of the Fundamental Theorem of Calculus, we can write the bias as

$$\begin{aligned}
\text{Err} - \text{Err}_p &= - \int_0^p \frac{\partial \text{Err}_t}{\partial t} dt = - \int_0^p 2 \sum_{i=1}^n \mu_i \mathbb{E}[D_\phi(\tilde{Y}_t, g(Y_t))] \\
&\quad - \frac{1}{(1-t)} \mathbb{E}[D_\phi(\tilde{Y}_t, g(Y_t))(\tilde{Y}_p + Y_p, 1)] dt \\
&= - \int_0^p 2 \sum_{i=1}^n \mu_i \text{Err}_t - \frac{1}{(1-t)} \text{Cov}[D_\phi(\tilde{Y}_t, g(Y_t)), \langle \tilde{Y}_p + Y_p, 1 \rangle] \\
&\quad - \frac{1}{(1-t)} 2 \text{Err}_t (1-t) \sum_{i=1}^n \mu_i dt \\
&= \int_0^p \frac{1}{(1-t)} \text{Cov}[D_\phi(\tilde{Y}_t, g(Y_t)), \langle \tilde{Y}_t + Y_t, 1 \rangle] dt \\
&= \int_0^p \frac{1}{(1-t)} \text{Corr}[D_\phi(\tilde{Y}_t, g(Y_t)), \langle \tilde{Y}_t + Y_t, 1 \rangle] \sqrt{\text{Var}[D_\phi(\tilde{Y}_t, g(Y_t))]} \sqrt{\text{Var}[\langle \tilde{Y}_t + Y_t, 1 \rangle]} dt \\
&= \int_0^p \frac{1}{(1-t)} \text{Corr}[D_\phi(\tilde{Y}_t, g(Y_t)), \langle \tilde{Y}_t + Y_t, 1 \rangle] \sqrt{\text{Var}[D_\phi(\tilde{Y}_t, g(Y_t))]} (2(1-t) \sum_{i=1}^n \mu_i)^{1/2} dt \\
&= \int_0^p \frac{1}{\sqrt{1-t}} \text{Corr}[D_\phi(\tilde{Y}_t, g(Y_t)), \langle \tilde{Y}_t + Y_t, 1 \rangle] \sqrt{\text{Var}[D_\phi(\tilde{Y}_t, g(Y_t))]} dt (2 \sum_{i=1}^n \mu_i)^{1/2}.
\end{aligned}$$

Upper bounding the correlation by 1 we have

$$\begin{aligned}
|\text{Err} - \text{Err}_p| &\leq \int_0^p \frac{1}{\sqrt{1-t}} \sqrt{\text{Var}[D_\phi(\tilde{Y}_t, g(Y_t))] dt} (2 \sum_{i=1}^n \mu_i)^{1/2} \\
&\leq \int_0^p \frac{1}{\sqrt{1-t}} \sqrt{\text{Var}[D_\phi(\tilde{Y}, g(Y))] + O(t)} dt (2 \sum_{i=1}^n \mu_i)^{1/2} \quad (\text{Assume } O(t) > 0) \\
&\leq \int_0^p \frac{1}{\sqrt{1-t}} (\sqrt{\text{Var}[D_\phi(\tilde{Y}, g(Y))] + O(\sqrt{t})}) dt (2 \sum_{i=1}^n \mu_i)^{1/2} \\
&= \sqrt{\text{Var}[D_\phi(\tilde{Y}, g(Y))]} (2 \sum_{i=1}^n \mu_i)^{1/2} \int_0^p \frac{1}{\sqrt{1-t}} dt \\
&\quad + (2 \sum_{i=1}^n \mu_i)^{1/2} \int_0^p \frac{1}{\sqrt{1-t}} O(\sqrt{t}) dt \\
&\leq p \sqrt{\text{Var}[D_\phi(\tilde{Y}, g(Y))]} (2 \sum_{i=1}^n \mu_i)^{1/2} + O(p^{3/2}) \quad (p \text{ small})
\end{aligned}$$

therefore, for small  $p$ , the bias decreases linearly to 0. Moreover, larger signal leads to higher bias and higher variance of the loss function  $\square$

## H.2 Proof of Proposition 3

The irreducible variance is defined as  $\text{Var}[\mathbb{E}[\widehat{\text{CB}}_p|Y]]$ . Note that this expectation is constant with respect to  $B$ , therefore we omit the bootstrap index from our calculations.

$$\begin{aligned}
\text{Var}[\mathbb{E}[\widehat{\text{CB}}_p|Y]] &= \text{Var}[\mathbb{E}[D_\phi(Y^*, g(Y^*)) + \langle \phi'(g(Y^*)), Y^* - Y^\dagger \rangle | Y]] \\
&= \text{Var}[\mathbb{E}[D_\phi(Y^*, g(Y^*)) + \langle \phi'(g(Y^*)), Y^* \rangle - \frac{(1-p)}{p} \langle \phi'(g(Y^*)), \omega \rangle | Y]] \\
&\leq 2\text{Var}[\mathbb{E}[D_\phi(Y^*, g(Y^*)) + \langle \phi'(g(Y^*)), Y^* \rangle | Y]] + 2\text{Var}[\frac{(1-p)}{p} \langle \phi'(g(Y^*)), \omega \rangle | Y]] \\
&\leq 2\text{Var}[D_\phi(Y, g(Y)) + \langle \phi'(g(Y)), Y \rangle] + O(p) + 2\text{Var}[\mathbb{E}[\frac{(1-p)}{p} \langle \phi'(g(Y^*)), \omega \rangle | Y]]. \quad (\text{LTV, Taylor})
\end{aligned}$$

Taking the limit,

$$\begin{aligned}
\lim_{p \rightarrow 0} \text{Var}[\mathbb{E}[\widehat{\text{CB}}_p|Y]] &\leq 2\text{Var}[D_\phi(Y, g(Y)) + \langle \phi'(g(Y)), Y \rangle] + 2 \lim_{p \rightarrow 0} \text{Var}[\mathbb{E}[\frac{(1-p)}{p} \langle \phi'(g(Y^*)), \omega \rangle | Y]] \\
&\leq 2\text{Var}[D_\phi(Y, g(Y)) + \langle \phi'(g(Y)), Y \rangle] + 2 \lim_{p \rightarrow 0} \mathbb{E}[\mathbb{E}^2[\frac{(1-p)}{p} \langle \phi'(g(Y^*)), \omega \rangle | Y]] \\
&\leq 2\text{Var}[D_\phi(Y, g(Y)) + \langle \phi'(g(Y)), Y \rangle] + 2 \lim_{p \rightarrow 0} \mathbb{E}[\mathbb{E}^2[\frac{(1-p)}{p} \langle \phi'(\tilde{g}(Y)), \omega \rangle | Y]] \quad (\tilde{g} \text{ is monotonic}) \\
&= 2\text{Var}[D_\phi(Y, g(Y)) + \langle \phi'(g(Y)), Y \rangle] + 2 \lim_{p \rightarrow 0} (1-p)^2 \mathbb{E}[(\langle \phi'(\tilde{g}(Y)), \mathbb{E}[\omega/p|Y] \rangle)^2] \\
&= 2\text{Var}[D_\phi(Y, g(Y)) + \langle \phi'(g(Y)), Y \rangle] + 2 \lim_{p \rightarrow 0} (1-p)^2 \mathbb{E}[(\langle \phi'(\tilde{g}(Y)), Y \rangle)^2] \\
&= 2\text{Var}[D_\phi(Y, g(Y)) + \langle \phi'(g(Y)), Y \rangle] + 2\mathbb{E}[(\langle \phi'(\tilde{g}(Y)), Y \rangle)^2].
\end{aligned}$$

### H.3 Proof of Proposition 4

*Proof.* We start from the fact that for  $B$  bootstrap samples,  $\text{Var}[\text{CB}_{p,B}|Y] = \text{Var}[\text{CB}_{p,1}|Y]/B$ . Then,

$$\begin{aligned}
\mathbb{E}[\text{Var}[\text{CB}_p|Y]] &= \mathbb{E}\left[\frac{1}{B}\text{Var}[D_\phi(Y^\dagger, g(Y^*)) + \phi(Y^*) - \phi(Y^\dagger)|Y]\right] \\
&= \mathbb{E}\left[\frac{1}{B}\text{Var}[\phi(Y^*) - \phi(g(Y^*)) - \langle \phi'(g(Y^*)), Y^\dagger - g(Y^*) \rangle |Y]\right] \\
&= \mathbb{E}\left[\frac{1}{B}\text{Var}[\phi(Y^*) - \phi(g(Y^*)) - \langle \phi'(g(Y^*)), Y^\dagger - Y^* + Y^* - g(Y^*) \rangle |Y]\right] \\
&= \mathbb{E}\left[\frac{1}{B}\text{Var}[D_\phi(Y^*, g(Y^*)) - \langle \phi'(g(Y^*)), Y^\dagger - Y^* \rangle |Y]\right] \\
&= \mathbb{E}\left[\frac{1}{B}\text{Var}[D_\phi(Y^*, g(Y^*)) - \frac{1}{p}\langle \omega, \phi'(g(Y^*)) \rangle + \langle \phi'(g(Y^*)), Y \rangle |Y]\right] \\
&\leq \frac{2}{B}\mathbb{E}[\text{Var}[D_\phi(Y^*, g(Y^*)) + \langle \phi'(g(Y^*)), Y \rangle |Y]] \\
&\quad + \frac{2}{Bp^2}\mathbb{E}[\text{Var}[\langle \omega, \phi'(g(Y^*)) \rangle |Y]] \\
&\leq \frac{2}{B}\text{Var}[D_\phi(Y^*, g(Y^*)) + \langle Y, \phi'(g(Y^*)) \rangle] + \frac{2}{Bp^2}\text{Var}[\langle \omega, \phi'(g(Y^*)) \rangle] \quad (\text{LTV}) \\
&= \frac{2}{B}\text{Var}[D_\phi(Y, g(Y)) + \langle Y, \phi'(g(Y)) \rangle] + \frac{2}{B}O(p) \\
&\quad + \frac{2}{Bp^2}\text{Var}[\langle \omega, \phi'(g(Y^*)) \rangle]. \quad (\text{Taylor})
\end{aligned}$$

For the last term, note that  $\omega \perp Y^*$ . Then, we can use that fact that if  $X_1$  and  $X_2$  are independent,  $\text{Var}[X_1X_2] = \text{Var}[X_1]\text{Var}[X_2] + \text{Var}[X_1]\mathbb{E}^2[X_2] + \text{Var}[X_2]\mathbb{E}^2[X_1]$ :

$$\begin{aligned}
\frac{2}{Bp^2}\text{Var}[\langle \omega, \phi'(g(Y^*)) \rangle] &= \frac{2}{Bp^2}\sum_{i=1}^n \text{Var}[\omega_i \phi'(g_i(Y^*))] \\
&= \frac{2}{Bp^2}\sum_{i=1}^n (\text{Var}[\omega_i]\text{Var}[\phi'(g_i(Y^*))] + \text{Var}[\omega_i]\mathbb{E}^2[\phi'(g_i(Y^*))] \\
&\quad + \text{Var}[\phi'(g_i(Y^*))]\mathbb{E}^2[\omega_i]) \\
&= \frac{2}{Bp^2}\sum_{i=1}^n (\mu_i p \text{Var}[\phi'(g_i(Y^*))] + \mu_i p \mathbb{E}^2[\phi'(g_i(Y^*))] + \text{Var}[\phi'(g_i(Y^*))]\mu_i^2 p^2) \\
&= \frac{2}{Bp}\sum_{i=1}^n \mu_i \mathbb{E}[\phi'(g_i(Y^*))^2] + \frac{2}{B}\sum_{i=1}^n \mu_i^2 \text{Var}[\phi'(g_i(Y^*))] \\
&= \frac{2}{Bp}\sum_{i=1}^n \mu_i \mathbb{E}[\phi'(g_i(Y^*))^2] + \frac{2}{B}\sum_{i=1}^n \mu_i^2 (\text{Var}[\phi'(g_i(Y^*))] + O(p)).
\end{aligned}$$

Putting it all together we get the desired result.  $\square$